Discovery of Potent and Selective Inhibitors of Human Reticulocyte 15-Lipoxygenase-1

Ganesha Rai,[†,§] Victor Kenyon,[‡,§] Ajit Jadhav,[†] Lena Schultz,[†] Michelle Armstrong,[‡] J. Brian Jameson, II,[‡] Eric Hoobler,[‡] William Leister,[†] Anton Simeonov,[†] Theodore R. Holman,*,[‡] and David J. Maloney*,[†]

[†]*NIH Chemical Genomics Center, National Human Genome Research Institute, National Institutes of Health, 9800 Medical Center Drive, MSC 3370, Bethesda, Maryland 20892, and* [‡]*Department of Chemistry and Biochemistry, University of California, Santa Cruz, 250 Physical Sciences Building, Santa Cruz, California 95064.* [§] *Both of these authors contributed equally to this work.*

There are a variety of lipoxygenases in the human body (hLO), each having a distinct role in cellular biology. Human reticulocyte 15-lipoxygenase-1 (15-hLO-1), which catalyzes the dioxygenation of 1,4-*cis,cis*-pentadiene-containing polyunsaturated fatty acids, is implicated in a number of diseases including cancer, atherosclerosis, and neurodegenerative conditions. Despite the potential therapeutic relevance of this target, few inhibitors have been reported that are both potent and selective. To this end, we have employed a quantitative high-throughput (qHTS) screen against ~74000 small molecules in search of reticulocyte 15-hLO-1 selective inhibitors. This screen led to the discovery of a novel chemotype for 15-hLO-1 inhibition, which displays nM potency and is > 7500-fold selective against the related isozymes, 5-hLO, platelet 12-hLO, epithelial 15-hLO-2, ovine cyclooxygenase-1, and human cyclooxygenase-2. In addition, kinetic experiments were performed which indicate that this class of inhibitor is tight binding, reversible, and appears not to reduce the active-site ferric ion.

Introduction

Lipoxygenases (LOs[a]) are nonheme, iron-containing enzymes found in both the plant and animal kingdoms. LOs catalyze the dioxygenation of 1,4-*cis,cis*-pentadiene-containing polyunsaturated fatty acids (e.g., linoleic acid (LA) and arachidonic acid (AA)) to form hydroperoxy-fatty acids.[1] The mechanism for this reaction is the abstraction of a hydrogen atom from the 1,4-*cis,cis*-pentadiene by an active site ferric ion.[2] Inhibitors of lipoxygenases can target this unique reaction via a variety of mechanisms such as reductive, chelation, competitive, and/or allosteric.[3]

Human lipoxygenases (hLOs) have been implicated in several diseases involving inflammation, immune disorders, and various types of cancers.[4−6] 5-hLO[7] has been implicated in cancer[3e,8] and asthma,[9] while platelet-type 12-LO[10] has been implicated in psoriasis[11] and pancreatic,[12] breast,[13,14] and prostate cancers.[15,16] Reticulocyte 15-hLO-1 (15-hLO-1) is less straightforward since it has been implicated both in resolving and promoting human disease.[17] In prostate tumors, cancer cells have a higher expression of 15-hLO-1 compared with normal adjacent tissue, and this expression positively correlates with the virulence of the tumor.[18−20] In contrast, 15-hLO-2 is expressed in normal prostate tissue, but poorly expressed in prostate tumors, with an inverse correlation with the virulence of the tumor.[21] This opposing effect between 15-hLO-1 and 15-hLO-2 is thought to be due to the difference in product generation. While one of the major 15-hLO-1 products, 13-(*S*)- hydroperoxy-9,11-(*Z,E*)-octadecadienoic acid (13-HPODE) from LA, up-regulates the MAP kinase signaling pathway, the major 15-hLO-2 product, 15-(*S*)-HPETE from AA, down-regulates MAP kinase. In colon cancer, however, 15-hLO-1 has been proposed to have a beneficial role. Downregulation of 15-hLO-1 is linked to colorectal tumorigenesis and restoring 15-hLO-1 expression in colon cancer in vivo xenografts downregulates antiapoptotic proteins and inhibits cell growth.[22]

Other potential therapeutic benefits of 15-hLO-1 inhibitors include asthma,[23] cardiovascular disease,[24] and minimizing the brain damage that occurs after a stroke. One of the major features of neuronal cell death after a stroke event is the accumulation of reactive oxygen species (ROS).[25] Recently, it has been reported that 15-hLO-1 damages the mitochondria, which leads to the breakdown of the membrane potential, the production of ROS, and cytochrome c release, suggesting that 15-hLO-1 is the central executioner in an oxidative stress-related neuronal death program.[26] These broad implications in disease regulation underscore the need for small molecule

*To whom correspondence should be addressed. For D.J.M.: Phone: 301-217-4381. Fax: 301-217-5736. E-mail: maloneyd@mail.nih.gov. For T.R.H: Phone: 831-459-5884. Fax: 831-459-2935. E-mail: holman@ucsc.edu.

[a] Abbreviations: LO, lipoxygenase; sLO-1, soybean lipoxygenase-1; 15-hLO-1, human reticulocyte 15-lipoxygenase-1; 15-hLO-2, human epithelial 15-lipoxygenase-2; 12-hLO, human platelet 12-lipoxygenase; 15-rLO, rabbit reticulocyte 15-lipoxygenase; COX, cyclooxygenase; NDGA, nordihydroguaiaretic acid; AA, arachidonic acid; 15-HPETE, 15-(*S*)-hydroperoxyeicosatetraenoic acid; 15-HETE, 15-(*S*)-hydroxyeicosatetraenoic acid; 12-HPETE, 12-(*S*)-hydroperoxyeicosatetraenoic acid; 12-HETE, 12-(*S*)-hydroxyeicosatetraenoic acid; LA, linoleic acid; 13-HPODE, 13-(*S*)-hydroperoxyoctadecadienoic acid; 13-HODE, 13-(*S*)-hydroxyoctadecadienoic acid; ALA, alpha-linolenic acid; 13-HPOTrE, 13-(*S*)-hydroperoxyoctadecatrienoic acid; V_{max}; maximal velocity (μmol/min); K_M, Henri−Michaelis−Menten constant (μM); [E], total active enzyme concentration; IC$_{50}$, inhibitor constant at 50% inhibition; K_i^{app}, apparent inhibition constant when [E] ≫ K_i^{app}; DPPH, 1.1-diphenyl-2-picrylhydrazyl; XO, xylenol orange; HTS, high-throughput screening; MLSMR, Molecular Libraries Small Molecule Repository; MLPCN, Molecular Libraries Probe Production Center Network; qHTS, quantitative high-throughput screening; CRC, concentration response curve; EDC, 1-ethyl-3-(3-dimethylaminopropyl)carbodiimide hydrochloride; BTAC, *N*-benzyl-triethylammonium chloride.

inhibitors against 15-hLO-1. However, to date, relatively few inhibitors have been reported that are both potent and selective.

Over the last 10 years, our laboratory[3a,27] and others[28−30] have attempted to identify potent and selective 15-hLO-1 inhibitors, but with limited success (submicromolar potency, with approximately 40-fold selectivity against 12-hLO). Unfortunately, the majority of these compounds are reductive inhibitors and/or are promiscuous polyphenolic/terpene based terrestrial natural products such as boswellic acid (**1**) (IC$_{50}$ = 1 μM),[28] hexamethoxyflavone (IC$_{50}$ = 50 μM),[29] nor-dihydroguaiaretic acid (NDGA) (IC$_{50}$ = 0.5 μM),[3a] baicalein (**2**)
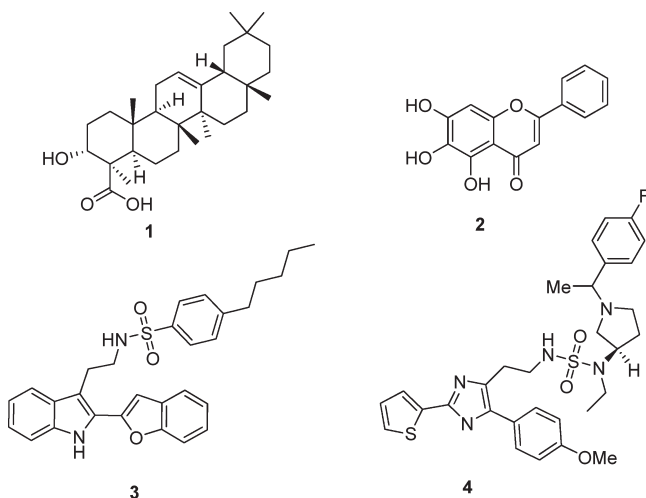
(IC$_{50}$ = 2 μM),[27a] and bacterial hopanoids (IC$_{50}$ = 10 μM).[30] The literature is also replete with other 15-LO inhibitors, but these have only been screened against sLO-1,[31−33] which has been found to be a poor model for 15-hLO-1 inhibition.[27a,b,34] Recently, we were able to identify nonreductive and selective inhibitors utilizing computational docking; however, the potency of these compounds were only in the low micromolar range.[35] The most promising 15-hLO-1 inhibitors thus far are the tryptamine[36] (**3**) and imidazole-based[37] (**4**) derivatives, which have low nanomolar potency and selectivity against both 5-hLO and 12-hLO (Figure 1).[38]

Given the limited number of potent and selective 15-hLO-1 inhibitors and the potential therapeutic benefit for such compounds, we sought to provide the scientific community with additional small molecule biochemical probes to study this important target. As such, we conducted a quantitative high-throughput screen (qHTS) in 1536-well format using a library containing 74290 small molecules[39] as part of the NIH Molecular Libraries Probe Production Center Network (MLPCN) in search of novel potent and selective 15-hLO-1 inhibitors. In this report, we discuss the discovery, synthesis, and structure−activity relationships (SAR) of a novel chemotype, which displayed nanomolar potency and is highly selective against 15-hLO-1. Moreover, preliminary investigations into the mechanism of action are presented.

Chemistry

Despite the fact that we screened a relatively large number of compounds belonging to a diverse chemical library, few hits exhibited potent and selective inhibition for 15-hLO-1. However, the 1,3,4-oxadiazole-2-thiol chemotype (**5**) (Figure 2D) showed potent (19 nM) inhibition against 15-hLO-1 and was selective against related isozymes (5-hLO, 12-hLO, and 15-hLO-2).
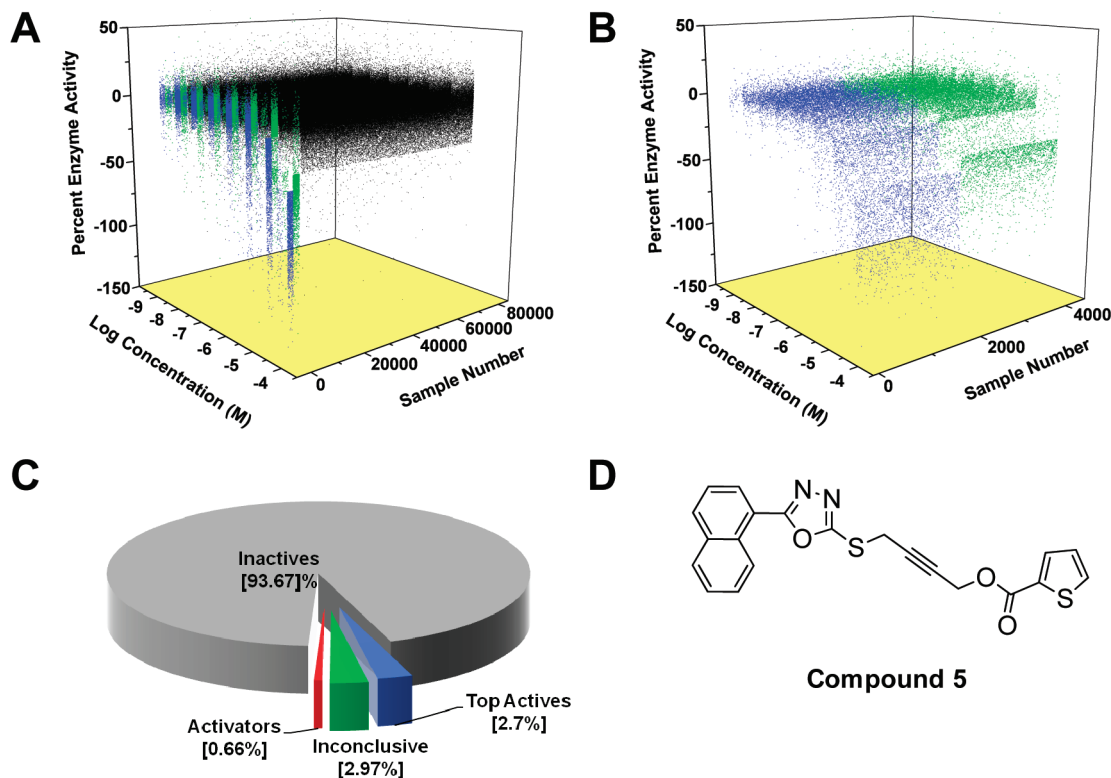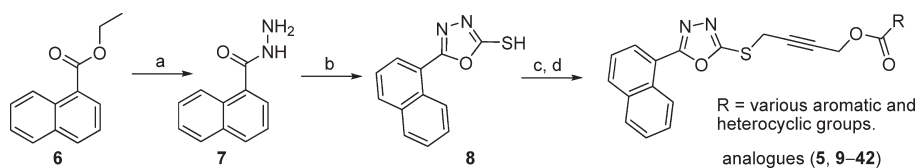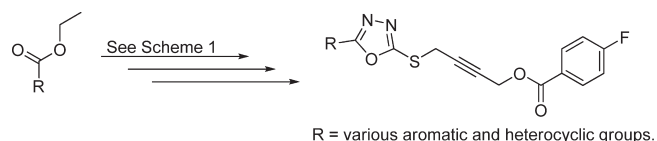

Figure 1. Representative examples of previously reported 15-hLO-1 inhibitors.

Figure 2. (A) qHTS concentration response profiles of 74290 compounds screened against 15-hLO-1. (B) Top actives from the primary screen are shown in blue, and inconclusive or weak inhibitors are shown in green. (C) Distribution of activity response in the primary screen. (D) The lead compound **5** from qHTS, which was chosen for optimization.

Scheme 1. Synthetic Route of Compounds **5, 9−43**[a]

R = various aromatic and heterocyclic groups.

analogues (**5, 9–42**)

[a] Reagents and conditions: (a) anhydrous hydrazine (5 equiv), EtOH, reflux, 16 h, 92%; (b) CS$_2$ (2.5 equiv), KOH (2.3 equiv), EtOH, reflux, 2 h, then acidified, 90%; (c) 4-chlorobut-2-yn-1-ol, K$_2$CO$_3$, acetone, reflux, 1 h, 86%; (d) EDC (2 equiv), cat. DMAP, various carboxylic acid derivatives (1.2 equiv), DMF, room temperature, 1 h.

R = various aromatic and heterocyclic groups.

Figure 3. Synthesis of Analogues **43−55**.

Moreover, this novel scaffold is chemically tractable and amenable to chemical modification at various positions of the molecule, allowing for rapid exploration of the SAR profile.

Our initial round of analogues was focused around modification of the 2-thiophene carboxylic acid moiety in our lead compound **5**. As such, the synthesis commenced with treatment of the commercially available ethyl 1-naphthoate (**6**) with anhydrous hydrazine in ethanol at reflux to afford the desired hydrazide **7** in high yield. (Scheme 1). Cyclization was accomplished using carbon disulfide in the presence of KOH in ethanol followed by acidification of the resulting thiolate to provide **8**. Alkylation of **8** with 4-chlorobut-2-yn-1-ol with K$_2$CO$_3$ in acetone provided the key propargylic alcohol intermediate from which a wide variety of ester derivatives (**9−42**) were prepared in a facile manner using EDC and cat. DMAP in DMF at room temperature.

The synthesis of analogues **43−55** was more laborious, as the divergent point for each analogue is in the first step of the sequence as shown in Figure 3. A variety of commercially available aromatic and heteroaromatic esters were carried through a similar synthetic route with one exception. To make the route as convergent as possible, 4-chlorobut-2-yn-1-ol was first coupled with either 2-thiophene carboxylic acid or 4-fluorobenzoic acid followed by subsequent coupling with intermediate **8** to provide the desired analogues **43−55**.
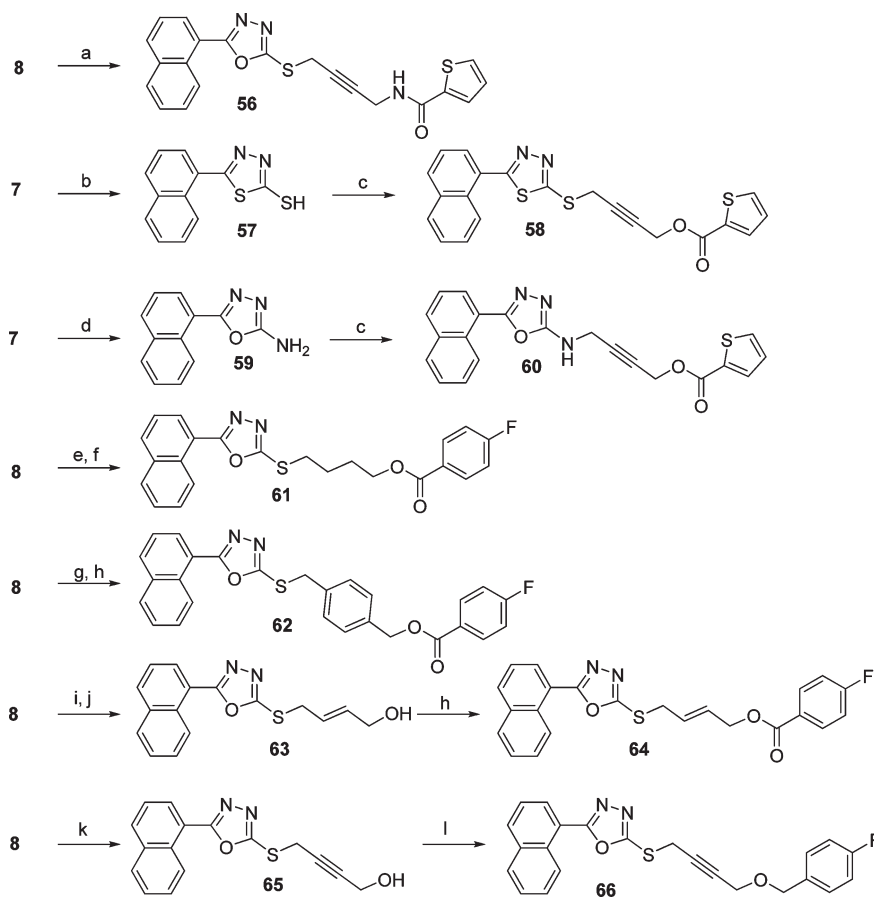
Last, we explored the effects of changing various heteroatoms throughout the core scaffold as well as altering the nature of the linker and terminal ester moiety. As such, the synthesis of the amide analogue **56** was accomplished via alkylation of **8** with *N*-(4-chlorobut-2-ynyl)thiophene-2-carboxamide using potassium carbonate in DMF as shown in Scheme 2. The requisite carboxamide was prepared using EDC mediated coupling of thiophene-carboxylic acid to commercially available 4-chlorobut-2-yn-1-amine. Analogues **58** and **60** were obtained from common intermediate **7**, either by treatment with carbon disulfide in the presence of KOH followed by cyclization with conc H$_2$SO$_4$ to provide the thiadiazole intermediate **57** or cyanogen bromide to give the oxadiazole 2-amine **59**, which upon alkylation with 4-chlorobut-2-ynyl thiophene-2-carboxylate afforded **58** and **60**, respectively. Synthesis of analogues **61** (alkyne reduced to alkane) and **62** (alkyne replaced with phenyl) involved alkylation of intermediate **8** with chloro-1-butanol and 4-(chloromethyl)benzyl alcohol, respectively, followed by EDC and cat. DMAP mediated esterification with 4-fluorobenzoic acid.

To further investigate the linker region, we attempted the synthesis of both the *Z*-alkene analogue and *E*-alkene analogue **64**, however, under several conditions, we found that the *Z*-olefin rapidly isomerized to the *E*-olefin so we were unable to isolate this compound. Synthesis of (*E*-alkene) **64** was achieved via alkylation of **8** with (*E*)-1,3-dichloropropene using *N*-benzyl-triethylammonium chloride (BTAC) and sodium hydroxide followed by hydrolysis using 0.1 M HCl/DMSO to afford the allylic alcohol **63**, which was esterified using standard conditions. Propargylic alcohol derivative **65** was synthesized by alkylation of **8** with 4-chlorobut-2-yn-1-ol, which was further modified using 4-fluorobenzyl bromide to provide compound **66**.

Results and Discussion

In the search for novel small molecule inhibitors, we performed a high-throughput screen, testing a diverse collection of 74290 compounds arrayed as dilution series. The 15-hLO-1 HTS assay utilized a colorimetric method for detecting the hydroperoxide reaction products of lipoxygenase.[40] The extent of product formation was monitored by a secondary chromogenic reaction in which Xylenol Orange (XO) binds to the ferric ions produced from the reaction between the hydroperoxide product and the ferrous ion added to the assay. The resulting Fe(III)−XO complex is characterized by a red-shifted absorbance in the 560−580 nm region (orange to purple color). The assay was initially developed for a 384-well format and further miniaturized to 4 μL enzymatic reaction volume in a 1536-well format. Enzyme and substrate concentrations, as well as reaction time, were optimized in order to achieve the highest signal-to-background ratio without reaching reaction plateau. The stability of working concentrations of the assay components, 15-hLO-1 enzyme, and substrate at +4 °C, and the chromogenic reagent FeXO prepared in dilute acid at room temperature permitted the implementation of an unattended overnight screening operation.

The full-collection screen utilized 463 assay plates run in an uninterrupted robotic screening sequence of approximately 52 h. The average signal-to-background ratio was 5.5 and the average *Z′* screening factor was 0.64 (Supporting Information Figure S1), indicating a robust performance of the screen. The known lipoxygenase inhibitor, nordihydroguaiaretic acid (NDGA), was included as an intraplate control on each assay plate (16-point dilution series in duplicate between 57.5 μM and 1.8 nM), to further ascertain screening quality. The resulting average IC$_{50}$ of NDGA was 0.283 ± 0.09 μM (n = 926) with a minimum significant ratio (defined by Eastwood et al.[41]) of 1.9, thus indicating a stable run (Supporting Information Figure S2). In the present screen, 74290 compounds were tested in at least seven concentrations, ranging from 57.5 μM to 0.7 nM; the screen yielded a range of active samples associated with different potencies (IC$_{50}$) and concentration−response curve (CRC) quality (Figure 2A,B).

Scheme 2. Synthetic Route for Compounds **56−66**

a Reagents and conditions: (a) *N*-(4-chlorobut-2-ynyl)thiophene-2-carboxamide (1.1 equiv), K$_2$CO$_3$ (5 equiv), DMF, 40 °C, 2 h; (b) CS$_2$ (2.3 equiv), KOH (1 equiv), EtOH, rt, 4 h, filter then add to conc H$_2$SO$_4$, 0 °C → rt, 2 h, 61%; (c) 4-chlorobut-2-ynyl thiophene-2-carboxylate (1.1 equiv), NaH (2 equiv), DMF, 0 °C, 1 h then rt, 5 h; (d) cyanogen bromide (1.2 equiv), EtOH, reflux, 1 h, 84%; (e) 4-chlorobutan-1-ol, (1.1 equiv), K$_2$CO$_3$ (4 equiv), DMF, 40 °C, 1.5 h, 63%; (f) 4-fluorobenzoic acid (1.1 equiv), EDC (1.5 equiv), cat. DMAP, DMF; (g) 4-(chloromethyl)benzyl alcohol, (1.1 equiv), K$_2$CO$_3$ (4 equiv), DMF; (h) 4-fluorobenzoic acid (1.1 equiv), EDC (1.5 equiv), cat. DMAP, DMF; (i) (*E*)-1,3-dichloropropene (1.5 equiv), BTAC (0.15 equiv), 1:1 (1% aq NaOH/CHCl$_3$), rt, 4 h; (j) 2:1 (0.1 M aq HCl/DMSO), rt; (k) 4-chlorobut-2-yn-1-ol, (1.1 equiv), K$_2$CO$_3$ (4 equiv), DMF, 40 °C, 1.5 h; (l) 4-fluorobenzyl bromide, (2.2 equiv), NaH (4 equiv), DMF, 10 h.

Following the qHTS, the CRC data were subjected to a classification scheme to rank the quality of the CRCs, as described by Inglese and co-workers.[42] Briefly, the CRCs were placed in four classes. Class 1 contains complete concentration−response curves showing both upper and lower asymptotes and R^2 values greater than 0.9. Class 2 contains incomplete CRCs lacking the lower asymptote and shows $r^2 > 0.9$. Class 3 curves are of the lowest confidence as they are defined by a single concentration point where the minimal acceptance activity is set 3 SD of the mean activity, calculated as described above. Finally, class 4 contains compounds that do not show any CRCs and are therefore classified as inactives. Of the 74290 screened compounds, 69447 were regarded as inactives (Figure 2C) and 3789 as inconclusive. There were 1054 compounds that were classified as actives, belonging to curve classes −1.1, −1.2, −2.1, or −2.2. The complete screening results have been made available in Pub-Chem (PubChem Assay ID 887). Selected compounds that were active in the primary screen, and associated with high-quality complete concentration−response curves (presence of both asymptotes and maximum efficacy of greater than 80% inhibition) were reacquired and tested in the original HTS assay to confirm activity. Prioritized hits were then further characterized in the standard cuvette-based kinetic assay for lipoxygenase activity, which measures product formation by monitoring the increase in absorbance at 234 nm.[40b] On the basis of the retest and the confirmatory cuvette-based kinetic measurements, a novel chemotype (compound **5**, Figure 2D), which displayed nM potency against the enzyme, and was inactive in enzymatic assays against the related isozymes 15-hLO-2, 12-hLO, and 5-hLO, was selected for further characterization.

To date, an X-ray structure of 15-hLO-1 has yet to be reported. However, crystallization of rabbit reticulocyte 15-LO (15-rLO), which has approximately 80% sequence identity with the human variant, has been achieved.[43] As mentioned above, utilization of a homology model based on the 15-rLO has been used successfully in the identification of 15-hLO-1 inhibitors and thus could be exploited in our investigations. However, initially we aimed to define the SAR profile through systematic modification of the various functional groups on the lead molecule **5** (Figure 2D). Our efforts toward this goal commenced with derivatization of the thiophene ester moiety. This position allows for rapid exploration of SAR via a late-stage esterification of a common intermediate (Scheme 1). As shown in Table 1, we prepared molecules with varying substitution on the thiophene core (analogues **9−11**), carbocycles (**13−15**, **18**), and various

Table 1. SAR of Various Ester Derivatives: Lead Compound **5** and Analogues (**9**−**23**)

Analogue	R	K_i^{app} (nM) [SD][a]
"hit" **5**	2-thiophene	19 [8]
9	2-(3,4,5-Cl-thiophene)	<10[b]
10	2-(3-Cl-thiophene)	<10
11	3-thiophene	<10
12	2-furan	170 [30]
13	cyclopropane	270 [10]
14	cyclobutane	85 [6]
15	cyclopentane	<10
16	4-1H-imidazole	1400 [300]
17	3-(2-fluoropyridine)	<10
18	2-naphthalene	22 [7]
19	2-benzofuran	15 [6]
20	4-indole	76 [7]
21	2-benzothiophene	<10
22	3-benzothiophene	<10
23	2-(3-chlorobenzothiophene)	31 [6]

[a] The inhibition data were fit as described in the Methods section, where the weak inhibitors (greater than 1 μM) were fit with a standard hyperbolic equation and the moderate inhibitors (1 μM to 10 nM) were fit using the Morrison equation. The potent inhibitors (less than 10 nM) could not be fit using the Morrison equation due to the high dependence of the K_i^{app} on active enzyme concentration. [b] Maximum inhibition was 60%.

heterocycles (**12**, **16**, **17**, **19**−**23**). Our first observation was that modification of this terminal ester moiety is well tolerated as the majority of the analogues maintained potency. It should be noted that due to limitations in assay detection and enzyme concentration, we are unable to accurately differentiate potencies lower than 10 nM, thus limiting our ability to evaluate SAR of these more potent analogues (see the Experimental Section for a more detailed explanation). Given that the potency of our lead compound **5** is near the limit of detection, we are not able to clearly define improved potency over the qHTS hit, however, we are able to determine which structural changes are not well tolerated and which compounds should be progressed into further studies. As such, some clear SAR trends emerged from the initial round of analogues, the first being that sulfur containing heterocycles appear to be preferred over their oxygen counterpart. This is highlighted by 2-thiophene analogue (**5**) and 2-furan analogue (**12**), which resulted in an 8-fold loss in activity (19−170 nM, respectively). Moreover, a moderate loss in potency was observed when comparing the 2-benzothiophene analogue **21** (<10 nM) and the corresponding 2-benzofuran derivative **19** (15 nM). Comparison of analogues **13**, **14**, and **15** reveals a preference for increased hydrophobicity in this portion of the binding pocket as potency improved proportionally to ring size (IC$_{50}$ = cyclopropane (**13**) > cyclobutane (**14**) > cyclopentane (**15**)). The most pronounced loss in potency was observed with the imidazole analogue **16**, which is approximately 70 times less active than the original lead **5** whereas the indole analogue **20** was approximately 4-fold less active, consistent with hydrophobicity playing an important role. Taken together, these results suggest that sulfur is preferred over oxygen in the heterocycle and that potency is generally improved with increased hydrophobicity of this moiety (*vide infra*).

Having explored various heterocyclic changes to the ester moiety, we turned our attention to benzoic acid derivatives, as we noticed that the simple benzoyl analogue (**24**) exhibited comparable if not improved potency to the lead compound **5** (<10 and 19 nM, respectively). As shown in Table 2, we explored various electron-donating and electron-withdrawing groups at different positions on the ring. Generally, all substitutions were well tolerated and relatively flat SAR was
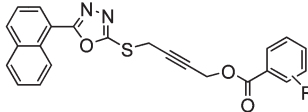
observed, which is to be expected given the results of our initial ester modifications (Table 1). While not explored in detail, it appears that ortho-substituted electron-donating groups are not favorable given the drastic loss in potency (470 nM) for analogue **33** (R = 2-OMe). However, this effect could also be a result of an unfavorable steric interaction of the 2-methoxy group disrupting a key hydrogen bond interaction of the carbonyl oxygen on the ester moiety.

Through these initial SAR investigations (see Tables 1 and 2), we learned that the terminal ester moiety is fairly amendable to substitution with hydrophobic groups and could possibly be exploited later to engineer a molecule with improved properties such as aqueous solubility.

We next investigated changes to the various heteroatoms throughout the core scaffold and also the "left-hand" portion of the molecule (i.e., naphthalene moiety). Replacing the naphthalene group with other carbocycles and heterocycles (analogues **43**−**55**) was generally well tolerated. Interestingly, analogues **43** (R = 2-naphthalene, <10 nM), **47** (R = 4-F-Ph, <10 nM), and **49** (R = 4-Cl-Ph, <10 nM) are more potent than the ortho-substituted analogues **45** (R = 2-F-Ph, 43 nM) and **48** (R = 2-Cl-Ph, 57 nM), which may suggest that the more linear analogues (**43**, **47**, and **49**) are able to acquire favorable interactions by extending into a hydrophobic region in the active site. Future efforts will aim to exploit this SAR by preparing analogues such as (R = *p*-bisphenyl) and (R = 6-quinoline or 2-quinoline) to test this binding hypothesis.
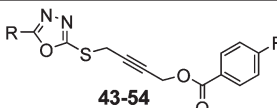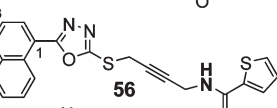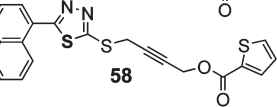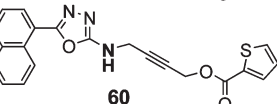
Unlike the relatively flat SAR observed for the ester modifications, variation of the heteroatoms throughout the core scaffold resulted in significant loss of potency in most cases, as shown in Table 3. Given the potential hydrolysis of modified ester derivatives by intracellular esterases, we first examined the more hydrolytically stable amide analogue **56**. However, this change resulted in a drastic loss in activity (100-fold), with the amide **56** having an IC$_{50}$ of 2 μM compared to the corresponding ester analogue **5** (IC$_{50}$ = 19 nM). For analogue **58**, in which the oxadiazole is changed to a thiadiazole, we also observe a loss in potency, but this analogue was noticeably less soluble, which complicated the biochemical characterization of this compound. We postulated that switching the sulfur for a nitrogen, at the 2-position of the

Table 2. SAR of Benzoic Acid Derivatives: Analogues (**24**−**42**)

Analogue	R	$K_i{}^{app}$(nM) [SD][a]	
24	H	<10	
25	2-F	<10	
26	3-F	<10	
27	4-F	<10	
28	2,4-F	<10	
29	3,4-F	<10	
30	3,4,5-F	16	[5]
31	4-Cl	<10	
32	4-Br	<10	
33	2-OMe	470	[70]
34	4-OMe	<10	
35	4-N(Me)$_2$	15	[6]
36	S(O)$_2$Me	33	[5]
37	4-SCF$_4$	<10	
38	4-OCF$_2$H	<10	
39	4-OCF$_3$	<10	
40	3-CF$_3$	27	[7]
41	4-CF$_3$	<10	
42	3-CF$_3$,4-Cl	100	[20]

[a] The inhibition data were fit as described in the Methods section, where the weak inhibitors (greater than 1 μM) were fit with a standard hyperbolic equation and the moderate inhibitors (1 μM to 10 nM) were fit using the Morrison equation. The potent inhibitors (less than 10 nM) could not be fit using the Morrison equation due to the high dependence of the $K_i{}^{app}$ on active enzyme concentration.

Table 3. SAR of Analogues (**43**−**56**, **58** and **60**)

Analogue	R	$K_i{}^{app}$(nM) [SD][a]	
43	2-naphthalene	<10	
44	Ph	26	[7]
45	2-F-Ph	43	[6]
46	3-F-Ph	<10	
47	4-F-Ph	<10	
48	2-Cl-Ph	57	[6]
49	4-Cl-Ph	<10	
50	2-Furan	1000	[50]
51	2-thiophene	82	[8]
52	2-OMe-Ph	81	[10]
53	2-naphthalene-3-ol	low solubility	
54	2-indole	23	[7]
55	5-quinoline	140	[6]
56	NA	2000	[500]
58	NA	low solubility	
60	NA	1300	[100]

[a] The inhibition data were fit as described in the Methods section, where the weak inhibitors (greater than 1 μM) were fit with a standard hyperbolic equation and the moderate inhibitors (1 μM to 10 nM) were fit using the Morrison equation. The potent inhibitors (less than 10 nM) could not be fit using the Morrison equation due to the high dependence of the $K_i{}^{app}$ on active enzyme concentration.
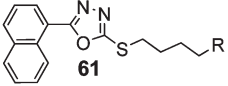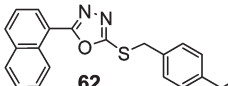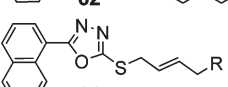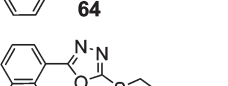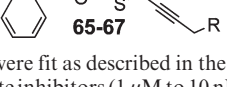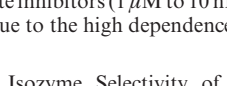
oxadiazole (analogue **60**), might result in an additional hydrogen-bond (donating) interaction; however, this too was unfavorable, with a potency of 1.3 μM being obtained. Accordingly, this SAR investigation indicates that linear hydrophobic moieties are favored for the "left-hand" portion of the molecule and other heterocycles in this position are relatively well tolerated, but heteroatom changes to the core structure are generally unfavorable.

Finally, we investigated the tolerance for changes in the linker region and the role of the carbonyl oxygen on the terminal ester moiety. Preliminary docking-based binding hypothesis of this chemotype in the active site of 15-hLO-1 suggested that the alkyne occupies a narrow constriction linking two hydrophobic pockets, presenting a "barbell-type" shape. To test this hypothesis, we synthesized alkane derivative (**61**), *E*-alkene (**64**), and replaced the alkyne moiety with a phenyl group (**62**), which should maintain the planar nature of the appended groups. As mentioned above, attempts to synthesize the Z-alkene derivative were unsuccessful, as under numerous conditions rapid isomerization to the seemingly more stable *E*-alkene occurred. As shown in Table 4, a moderate loss of potency was observed for alkane derivative **61** (600 nM), however, the *E*-alkene analogue (**64**) had almost no loss in potency (26 nM) compared to the alkyne (19 nM). In contrast, complete loss in activity occurred with the phenyl analogue **62** (>100 μM), suggesting that while the alkyne moiety is not required for activity, more bulky linkers (i.e., switching alkyne for phenyl) are unfavorable, presumably because they cannot fit within a narrow region in the active site.

We next synthesized the ether analogue **66** to investigate the importance of the ester carbonyl and observed complete loss in activity, indicating the necessity of a hydrogen bond acceptor in this position. Additionally, this key interaction appears to be easily disrupted, as was seen with the loss of activity with the ortho-substituted benzoic acid derivative **33** and the amide **56**. The ketone analogue **67** was also prepared but unfortunately had reduced solubility, which hampered the ability to obtain an accurate IC$_{50}$. Given the apparent

Table 4. SAR of Analogues (**61**, **62**, **64**−**67**)

Analogue	R	K_i^{app}(nM) [SD]^a
61	4-fluorobenzoic acid	600 [100]^b
62	4-fluorobenzoic acid	>70000
64	4-fluorobenzoic acid	26 [16]
65	OH	3500 [300]
66	4-fluorobenzyl alcohol	>100000
67	$CH_2C(O)Ph$	low solubility

^{a} The inhibition data were fit as described in the Methods section, where the weak inhibitors (greater than 1 μM) were fit with a standard hyperbolic equation and the moderate inhibitors (1 μM to 10 nM) were fit using the Morrison equation. The potent inhibitors (less than 10 nM) could not be fit using the Morrison equation due to the high dependence of the K_i^{app} on active enzyme concentration. ^{b} Maximum inhibition was 70%.

Table 5. Lipoxygenase Isozyme Selectivity of the Top 15-hLO-1 Inhibitors

analogue	15-hLO-1^a	15-hLO-2^a	12-hLO^a	5-hLO^a
5	0.019	>100	>100	>15
11	<0.010	>100	>100	>15
21	<0.010	>100	>100	>75
24	<0.010	>100	>100	>20
26	<0.010	>100	>100	>50
29	<0.010	>100	>100	>30
39	<0.010	>100	>100	>15
41	<0.010	>100	>100	>30
43	<0.010	>100	>100	>10
49	<0.010	>100	>100	>75

^{a} IC$_{50}$ values are reported in μM and estimated from three inhibitor concentrations, due to their lack of potency.

necessity of a hydrogen-bond acceptor at this position and our interest in improving the inherent stability of the lead molecule, we also prepared several ester bioisosteres which we expected would be more hydrolytically stable yet maintain potency. These analogues included 1,2,4- and 1,3,4-oxadiazoles, sulfonamides, and reversed esters, however, the potency of these derivatives was greatly decreased, with none having an IC$_{50}$ of less than 1 μM (data not shown).

With the commencement of our initial rounds of SAR explorations, which provided compounds with low nM potency against 15-hLO-1, we were then eager to determine the selectivity of our top analogues against related hLO isozymes (5-hLO, 12-hLO, and 15-hLO-2). Gratifyingly, all of our most potent analogues displayed excellent selectivity against all three isozymes, with only 5-hLO having IC$_{50}$ values below 100 μM (Table 5). These results were quite encouraging, as few compounds reported in the literature have achieved both nM potency toward 15-hLO-1 and selectivity against other isozymes, with the exception of chemotypes **3** and **4** (Figure 1). In addition, we explored whether this chemotype could inhibit cyclooxygenase-1 (COX-1) and/or COX-2 and found that compound **5** did not inhibit either COX at 10 μM (inhibition less than 5% of total activity), demonstrating a selectivity of greater than 1000-fold for this chemotype against 15-hLO-1 over either COX-1 or COX-2.

As previously mentioned, the X-ray structure of 15-hLO-1 has yet to be reported, therefore, several biochemical methods were employed to test the mechanism of inhibition for this

class of compounds. To ensure that the inhibition was not an effect of small molecule aggregates, the concentration of Triton X-100 was varied from 0.005% to 0.02%, with no change in the K_i^{app} for compound **5** witnessed.[44] To investigate if the inhibition resulted from reduction of the active site iron, DPPH, a free radical scavenger, was incubated with a representative group of inhibitors, and no reduction of the DPPH was observed (NDGA was used as a positive control). Additionally, there was no elongation of enzymatic lag phase or resumption of activity over time when these inhibitors were used, suggestive of a nonreductive inhibitory mechanism. A competitive substrate experiment was also performed to probe if the inhibition was allosteric in nature, but no change in product distribution was observed.[3d]

To investigate the reversibility of inhibition, 15-hLO-1 was incubated with the low nanomolar inhibitor **25**, the less potent **33** and an equivalent volume of DMSO as a positive control. After 10 min of incubation, the control displayed activity, whereas activity was abolished in the samples with inhibitor present. All three samples were then dialyzed for 2 h. Upon checking the activity of the three samples, activity had been restored in the samples with inhibitor present, indicating that the inhibition is a reversible process.

Steady-state kinetics were performed using compound **16** by monitoring the formation of 15-HPETE as a function of substrate and inhibitor concentration in the presence of 0.01% Triton X-100. Replots of K_M/V_{max} and $1/V_{max}$ versus inhibitor concentration (Supporting Information, Figures S3 and S4) yielded linear plots, with K_i equaling $0.87 \pm 0.07 \mu$M and K_i' equaling $8.1 \pm 0.9 \mu$M, which are defined as the equilibrium constants of dissociation from the catalytic and secondary sites, respectively. The secondary site could be the allosteric site due to its approximately 100-fold difference in binding from the catalytic site, which is consistent with our previous studies of 15-hLO-2,[45] however, no change in substrate preference was observed when inhibitor was added to 15-hLO-1 (*vide supra*). It should be noted that we were not able to determine the inhibitor mechanism for the more potent inhibitors due to the small K_i^{app} to enzyme ratio, however, we assume their mechanisms are comparable due to their similar structures.

Conclusion

An HTS campaign of ∼74290 compounds, aimed at identifying small molecule 15-hLO-1 inhibitors, uncovered the

5-substituted-1,3,4-oxadiazole-2-thiol chemotype, which was further optimized and elaborated through synthetic efforts to provide potent and selective inhibitors of 15-hLO-1. Modifications of the core scaffold helped us develop an SAR profile. Replacement of the thiophene and naphthalene moieties of the lead compound **5** with other aromatic and heteroaromatic groups was well tolerated. Consideration of the binding site and SAR of key analogues indicate the presence of a "barbell-like" binding pocket, which helps explain the requirement of a narrow linker region between the oxadiazole and terminal ester groups. Gratifyingly, our best compounds are potent (single digit nM) and exhibit > 7500-fold selectivity over similar hLO isozymes (5, 12, and 15-hLO-2) and COX isozymes. Additionally, this class of compounds was found to be nonreductive and exhibited reversible inhibition, with inhibitor binding occurring at both the catalytic site and possibly the allosteric site. Current efforts are focused on utilizing these molecules in cell-based systems across several therapeutic areas including cancer and stroke models. These results, along with other ongoing investigations, will be reported in due course. It is our hope that these reagents will provide a general, molecular tool to validate 15-hLO-1 as a therapeutic target.

Experimental Section

General Chemistry. Unless otherwise stated, all reactions were carried out under an atmosphere of dry argon or nitrogen in dried glassware. Indicated reaction temperatures refer to those of the reaction bath, while room temperature (rt) is noted as 25 °C. All solvents were of anhydrous quality, purchased from Aldrich Chemical Co. and used as received. Commercially available starting materials and reagents were purchased from Aldrich and were used as received.

Analytical thin layer chromatography (TLC) was performed with Sigma Aldrich TLC plates (5 cm × 20 cm, 60 Å, 250 μm). Visualization was accomplished by irradiation under a 254 nm UV lamp. Chromatography on silica gel was performed using forced flow (liquid) of the indicated solvent system on Biotage KP-Sil prepacked cartridges and using the Biotage SP-1 automated chromatography system. ^{1}H and ^{13}C NMR spectra were recorded on a Varian Inova 400 MHz spectrometer. Chemical shifts are reported in ppm, with the solvent resonance as the internal standard (CDCl$_3$ 7.26 ppm, 77.00 ppm, DMSO-d_6 2.49 ppm, 39.51 ppm for ^{1}H, ^{13}C, respectively). Data are reported as follows: chemical shift, multiplicity (s = singlet, d = doublet, t = triplet, q = quartet, brs = broad singlet, m = multiplet), coupling constants, and number of protons. Low resolution mass spectra (electrospray ionization) were acquired on an Agilent Technologies 6130 quadrupole spectrometer coupled to the HPLC system. High resolution mass spectral data was collected in-house using an Agilent 6210 time-of-flight mass spectrometer, also coupled to an Agilent Technologies 1200 series HPLC system. If needed, products were purified via a Waters semipreparative HPLC equipped with a Phenomenex Luna C18 reverse phase (5 μm, 30 mm × 75 mm) column having a flow rate of 45 mL/min. The mobile phase was a mixture of acetonitrile (0.025% TFA) and H$_2$O (0.05% TFA), and the temperature was maintained at 50 °C.

Samples were analyzed for purity on an Agilent 1200 series LC/MS equipped with a Luna C18 reverse phase (3 μm, 3 mm × 75 mm) column having a flow rate of 0.8−1.0 mL/min over a 7 min gradient and a 8.5 min run time. Purity of final compounds was determined to be >95%, using a 3 μL injection with quantitation by AUC at 220 and 254 nm (Agilent diode array detector).

General Procedure for the Syntheses of Aryl Hydrazides (Scheme 1). To a solution containing the aryl ester (10 mmol) in absolute ethanol (50 mL) was added anhydrous hydrazine (50 mmol), and the reaction mixture was refluxed overnight. The solid which precipitated upon cooling was collected by filtration. The collected precipitate was washed with water, then cold ethanol, and dried to provide aryl hydrazides (yield: 89−92%). The products were used without further purification.

General Procedure for the Formation of 2-Aryl-5-mercapto-1,3,4-oxadiazoles (Scheme 1). Potassium hydroxide (40 mmol) was dissolved in ethanol (50 mL), and then aryl hydrazide (17 mmol) and carbon disulfide (42 mmol) were added. The reaction mixture was heated at reflux for 2 h. Solvent was evaporated, and the residue was acidified with 10% HCl. The precipitate was collected by filtration, washed with water, and dried (88−99%). The product(s) were used without further purification.

5-(Naphthalen-1-yl)-1,3,4-oxadiazole-2-thiol (8). ^{1}H NMR (DMSO-d_6) δ 7.63−7.77 (m, 3 H), 8.06−8.16 (m, 2 H), 8.22 (d, J = 8.2 Hz, 1H), and 8.83 (dd, J = 8.5 and 1.1 Hz, 1H). ^{13}C NMR (DMSO-d_6) δ 118.51, 124.81, 125.32, 126.87, 128.35, 128.51, 128.62, 129.01, 132.96, 133.34, 160.30 and 176.90. HRMS (m/z): [M + H]$^+$ calcd for C$_{12}$H$_9$N$_2$OS, 229.0430; found, 229.0432.

4-(5-(Naphthalen-1-yl)-1,3,4-oxadiazol-2-ylthio)but-2-yn-1-ol (65). A solution of 5-(naphthalen-1-yl)-1,3,4-oxadiazole-2-thiol (**8**) (10 mmol), 4-chlorobut-2-yn-1-ol (10.2 mmol), and potassium carbonate (50 mmol) in acetone (50 mL) was refluxed for 1 h. The reaction mixture was filtered, and the filtrate was evaporated via reduced pressure. The crude residue was purified on a Biotage silica gel column. Elution with 30% ethyl acetate in hexanes gave the product. Yield: 86%. ^{1}H NMR (DMSO-d_6) δ 4.09 (dd, J = 5.6 and 2.4 Hz, 2 H), 4.29−4.33 (m, 2H), 5.21 (td, J = 5.8 and 2.4 Hz, 1 H), 7.63−7.78 (m, 3 H), 8.09 (d, J = 8.0 Hz, 1 H), 8.18−8.24 (m, 2 H), and 9.03 (d, J = 8.6 Hz, 1 H). ^{13}C NMR (DMSO-d_6) δ 21.18, 48.99, 78.61, 84.04, 119.27, 125.29, 125.36, 126.84, 128.28, 128.68, 128.90, 128.98, 132.72, 133.39, 162.48 and 165.37. HRMS (m/z): [M + H]$^+$ calcd for C$_{16}$H$_{13}$N$_2$O$_2$S, 297.0692; found, 297.0691.

4-(5-(Naphthalen-1-yl)-1,3,4-oxadiazol-2-ylthio)but-2-ynyl Thiophene-2-carboxylate (5). A solution of alcohol **65** (0.20 mmol), 2-thiophene carboxylic acid (0.22 mmol), EDC (0.40 mmol), and DMAP (0.10 mmol) in DMF (1 mL) was stirred at room temperature for 1 h. The product was purified directly by preparative HPLC (see General Chemistry for details). LC-MS: rt (min) = 6.91. ^{1}H NMR (CDCl$_3$) δ 4.15−4.22 (m, 2 H), 4.89−4.96 (m, 2 H), 7.03−7.10 (m, 1 H), 7.51−7.64 (m, 3 H), 7.64−7.74 (m, 1 H), 7.77−7.84 (m, 1 H), 7.93 (d, J = 8.2 Hz, 1 H), 8.03 (d, J = 8.2 Hz, 1 H), 8.14 (dd, J = 7.3 and 1.1 Hz, 1 H) and 9.18 (d, J = 8.6 Hz, 1 H). ^{13}C NMR (CDCl$_3$) δ 21.45, 52.69, 78.61, 80.55, 119.86, 124.81, 126.06, 126.73, 127.77, 128.18, 128.34, 128.64, 129.78, 132.61, 132.71, 132.99, 133.75, 134.08, 161.33, 162.44, and 166.17. HRMS (m/z): [M + H]$^+$ calcd for C$_{21}$H$_{15}$N$_2$O$_3$S$_2$, 407.0519; found, 407.0517.

N-(4-Chlorobut-2-ynyl)thiophene-2-carboxamide. A mixture of thiophene-2-carboxylic acid (1.0 g, 7.8 mmol) and EDC (2.2 g, 11.7 mmol) in CH$_2$Cl$_2$ (40 mL) was stirred for 30 min, and 4-chlorobut-2-yn-1-aminium chloride hydrochloride (1.3 g, 8.6 mmol) was added and stirred at room temperature for 2 h. The reaction mixture was diluted with dichloromethane and washed with water. The organic layer was dried over sodium sulfate. The crude residue was purified on a Biotage silica gel column. Elution with 20% ethyl acetate in hexanes gave the product. Yield: 1.32 g (79%). ^{1}H NMR (DMSO-d_6) δ 4.13 (dt, J = 5.6 and 2.1 Hz, 2 H), 4.46 (t, J = 2.0 Hz, 2 H), 7.15 (dd, J = 4.9 and 3.7 Hz, 1 H), 7.74−7.80 (m, 2 H) and 8.97 (t, J = 5.5 Hz, 1 H). ^{13}C NMR (DMSO-d_6) δ 28.47, 31.07, 77.21, 83.81, 127.97, 128.45, 131.19, 139.14, and 160.84. HRMS (m/z): [M + H]$^+$ calcd for C$_9$H$_9$ClNOS, 214.0088; found, 214.0090.

N-(4-(5-(Naphthalen-1-yl)-1,3,4-oxadiazol-2-ylthio)but-2-ynyl)-thiophene-2-carboxamide (56). To a mixture of **8** (0.040 g, 0.18 mmol) and N-(4-chlorobut-2-ynyl)thiophene-2-carboxamide (0.041 g, 0.19 mmol) in DMF (1 mL) was added potassium carbonate (0.12 g, 0.88 mmol) and was stirred at 40 °C for 2 h.

The resulting crude product was purified by preparative HPLC (see General Chemistry for HPLC purification conditions). LC-MS: rt (min) = 6.15. ^{1}H NMR (CDCl$_3$) δ 4.12 (t, J = 2.2 Hz, 2 H), 4.27 (dt, J = 5.3 and 2.2 Hz, 2 H), 6.30−6.39 (m, 1 H), 7.03 (dd, J = 4.9 and 3.7 Hz, 1 H), 7.46 (dd, J = 5.1 and 1.2 Hz, 1 H), 7.52−7.57 (m, 2 H), 7.57−7.64 (m, 1 H), 7.68 (ddd, J = 8.5, 6.9, and 1.4 Hz, 1 H), 7.90−7.95 (m, 1 H), 8.03 (d, J = 8.2 Hz, 1 H), 8.13 (dd, J = 7.3 and 1.3 Hz, 1 H), and 9.19 (dd, J = 8.6 and 0.8 Hz, 1 H). ^{13}C NMR (CDCl$_3$) δ 21.03, 21.56, 29.95, 80.44, 119.87, 124.84, 126.04, 126.75, 127.62, 128.19, 128.34, 128.49, 128.68, 129.78, 130.33, 132.74, 133.78, 138.01, 161.48, 162.50 and 166.23. HRMS (m/z): [M + H]$^+$ calcd for C$_{21}$H$_{16}$N$_3$O$_3$S, 406.0678; found, 406.0675.

2-(1-Naphthyl)-5-mercapto-1,3,4-thiadiazole (57). 1-Naphtho-hydrazide (**7**) (4.0 g, 21.5 mmol) and potassium hydroxide (1.2 g, 21.5 mmol) in ethanol (100 mL) was stirred for 30 min, and then carbon disulfide (3.0 mL, 49.4 mmol) was added. The reaction mixture was stirred at room temperature for 4 h. The yellow precipitate was collected by filtration, and the product was washed with ether. This product was slowly added to sulfuric acid (20 mL, 375 mmol) at 0 °C and then stirred at rt for 2 h. The reaction mixture was poured into ice, and the product was collected by filtration. Recrystallization from ethanol gave pure yellow product (3.2 g, 61%). ^{1}H NMR (DMSO-d_6) δ 7.60−7.74 (m, 3 H), 7.81 (d, J = 7.2 Hz, 1 H), 8.07 (d, J = 7.8 Hz, 1 H), 8.16 (d, J = 8.2 Hz, 1 H) and 8.60 (d, J = 8.2 Hz, 1 H). ^{13}C NMR (DMSO-d_6) δ 124.69, 124.98, 125.42, 126.87, 128.07, 128.78, 129.16, 129.55, 131.83, 133.46, 161.13, and 174.68. HRMS (m/z): [M + H]$^+$ calcd for C$_{12}$H$_9$N$_2$S$_2$, 245.0202; found, 245.0204.

4-(5-(Naphthalen-1-yl)-1,3,4-thiadiazol-2-ylthio)but-2-ynyl Thiophene-2-carboxylate (58). To a solution of **57** (0.20 mmol) in DMF (1 mL) at 0 °C was added NaH (0.40 mmol) followed by 4-chlorobut-2-ynyl thiophene-2-carboxylate (0.22 mmol), the reaction mixture was stirred at 0 °C for 1 h and then at room temperature for 5 h. The product was purified in a preparative HPLC (see General Chemistry for details). LC-MS: rt (min) = 7.10. ^{1}H NMR (CDCl$_3$) δ 4.23 (t, J = 2.2 Hz, 2 H), 4.89−4.96 (m, 2 H), 7.02−7.08 (m, 1 H), 7.50−7.65 (m, 4 H), 7.73−7.78 (m, 1 H), 7.80−7.84 (m, 1 H), 7.91−7.95 (m,1 H), 8.00 (d, J = 8.2 Hz, 1 H) and 8.68−8.76 (m, 1 H). ^{13}C NMR (CDCl$_3$) δ 22.55, 52.72, 78.49, 81.02, 93.24, 109.67, 124.89, 125.55, 126.66, 127.70, 127.77, 127.78, 128.39, 129.63, 129.68, 130.35, 131.47, 132.87, 133.84, 133.98, 161.27, 163.72, and 164.67. HRMS (m/z): [M + Na]$^+$ calcd for C$_{21}$H$_{15}$N$_2$O$_2$S$_3$, 445.0108; found, 445.0107.

2-(1-Naphthyl)-5-amino-1,3,4-oxadiazole (59). A mixture of 1-naphthohydrazide (**7**) (2.0 g, 10.7 mmol) and cyanogen bromide (1.4 g, 13 mmol) in EtOH (107 mL) was heated at reflux for 1 h. The solvent was removed, and the product was purified by recrystallization from ethanol to yield 1.9 g (84%) of pure product **59**. ^{1}H NMR (DMSO-d_6) δ 7.36 (s, 2 H), 7.59−7.71 (m, 3 H), 7.95−7.99 (m, 1 H), 8.03 (d, J = 8.0 Hz, 1 H), 8.08 (d, J = 8.2 Hz, 1 H), and 9.13 (d, J = 8.6 Hz, 1H). ^{13}C NMR (DMSO-d_6) δ 120.62, 125.35, 125.80, 126.44, 126.57, 127.68, 128.69, 128.91, 130.96, 133.48, 157.28, and 163.52.

4-(5-(Naphthalen-1-yl)-1,3,4-oxadiazol-2-ylamino)but-2-ynyl Thiophene-2-carboxylate (60). To a solution of 5-(naphthalen-1-yl)-1,3,4-oxadiazol-2-amine (**59**) (0.23 g, 1.1 mmol) in DMF (3 mL) was added NaH (0.07 g, 2.2 mmol) and stirred for 1 h at 0 °C, and then 4-chlorobut-2-ynyl thiophene-2-carboxylate (0.26 g, 1.2 mmol) was added. The reaction mixture was stirred for 5 h at room temperature and then product was poured into satd NH$_4$Cl (aq) and extracted with ethyl acetate, washed with water and then brine, and dried (MgSO$_4$). The crude product was purified in HPLC. LC-MS: rt (min) = 4.80. ^{1}H NMR (DMSO-d_6) δ 5.09 (d, J = 2.0 Hz, 2 H), 5.21 (d, J = 1.4 Hz, 2 H), 7.24−7.26 (m, 1 H), 7.68−7.81 (m, 3 H), 7.85−7.87 (m, 1 H), 8.01−8.03 (m, 1 H), 8.07−8.10 (m, 1 H), 8.15 (d, J = 8.0 Hz, 1 H), 8.32 (d, J = 8.4 Hz, 1 H), 8.77−8.83 (m, 1 H) and 10.45 (brs, 1H). HRMS (m/z): [M + H]$^+$ calcd for C$_{21}$H$_{16}$N$_3$-O$_3$S, 390.0907; found, 390.0912.

4-(5-(Naphthalen-1-yl)-1,3,4-oxadiazol-2-ylthio)but-2-ynyl Benzofuran-2-carboxylate (19). LC-MS: rt (min) = 7.05. ^{1}H NMR (DMSO-d_6) δ 4.40 (t, J = 2.1 Hz, 2 H), 5.06 (t, J = 2.0 Hz, 2 H), 7.31−7.40 (m, 1 H), 7.51 (ddd, J = 8.4, 7.1, and 1.3 Hz, 1 H), 7.61−7.69 (m, 4 H), 7.69−7.77 (m, 2 H), 8.06 (d, J = 8.0 Hz, 1 H), 8.13−8.23 (m, 2 H), and 9.03 (dd, J = 8.7 and 0.9 Hz, 1 H). ^{13}C NMR (DMSO-d_6) δ 20.95, 52.73, 52.97, 77.85, 82.44, 112.10, 114.81, 119.22, 123.26, 124.04, 125.26, 125.29, 126.41, 126.80, 128.14, 128.24, 128.59, 128.87, 128.94, 132.68, 144.10, 155.05, 157.79, 162.26, and 165.44. HRMS (m/z): [M + H]$^+$ calcd for C$_{25}$H$_{17}$N$_2$O$_4$S, 441.0904; found, 441.0907.

4-(5-(Naphthalen-1-yl)-1,3,4-oxadiazol-2-ylthio)but-2-ynyl 1H-Indole-4-carboxylate (20). LC-MS: rt (min) = 6.70. ^{1}H NMR (CDCl$_3$) δ 4.20 (t, J = 2.1 Hz, 2 H), 5.03 (t, J = 2.1 Hz, 2 H), 7.17−7.23 (m, 2 H), 7.31−7.36 (m, 1 H), 7.50−7.61 (m, 3 H), 7.67 (ddd, J = 8.5, 6.9, and 1.4 Hz, 1 H), 7.92 (dd, J = 7.6 and 1.0 Hz, 2 H), 8.01 (d, J = 8.2 Hz, 1 H), 8.13 (dd, J = 7.3 and 1.3 Hz, 1 H), 8.43 (br s, 1 H), and 9.19 (dd, J = 8.5 and 0.9 Hz, 1 H). ^{13}C NMR (CDCl$_3$) δ 21.56, 52.30, 79.31, 80.07, 103.94, 116.31, 119.96, 120.63, 121.11, 123.77, 124.84, 126.12, 126.47, 126.72, 127.51, 128.16, 128.33, 128.63, 129.81, 132.64, 133.77, 136.53, 162.51, 166.17, and 166.65. HRMS (m/z): [M + H]$^+$ calcd for C$_{25}$H$_{18}$N$_3$O$_3$S, 440.1069; found, 440.1064.

4-(5-(Naphthalen-1-yl)-1,3,4-oxadiazol-2-ylthio)but-2-ynyl 4-Fluorobenzoate (27) (aka ML094). LC-MS: rt (min) = 7.12. ^{1}H NMR (CDCl$_3$) δ 4.18 (t, J = 2.2 Hz, 2 H), 4.94 (t, J = 2.1 Hz, 2 H), 7.01−7.10 (m, 2 H), 7.51−7.63 (m, 2 H), 7.68 (td, J = 7.7 and 1.4 Hz, 1 H), 7.93 (d, J = 8.0 Hz, 1 H), 8.03 (dt, J = 8.9 and 2.7 Hz, 3 H), 8.13 (dd, J = 7.3 and 1.1 Hz, 1 H), and 9.19 (d, J = 8.6 Hz, 1 H). ^{13}C NMR (CDCl$_3$); δ 21.45, 52.75, 78.64, 80.57, 115.42, 115.63, 119.89, 124.78, 126.07, 126.73, 128.16, 128.25, 128.63, 129.75, 132.26, 132.36, 132.67, 133.75, 162.29, 164.60, 164.74, 166.16, and 167.13. HRMS (m/z): [M + H]$^+$ calcd for C$_{23}$H$_{16}$FN$_2$O$_3$S, 419.0865; found, 419.0864.

4-(5-(Naphthalen-1-yl)-1,3,4-oxadiazol-2-ylthio)but-2-ynyl 4-Chlorobenzoate (31). LC-MS: rt (min) = 7.38. ^{1}H NMR (CDCl$_3$) δ 4.18 (t, J = 2.1 Hz, 2 H), 4.94 (t, J = 2.2 Hz, 2 H), 7.35 (m, 2 H), 7.58 (m, 2 H), 7.68 (ddd, J = 8.6, 6.9, and 1.6 Hz, 1 H), 7.93 (m, 3 H), 8.03 (d, J = 8.2 Hz, 1 H), 8.13 (dd, J = 7.3 and 1.3 Hz, 1 H), and 9.19 (dd, J = 8.6 and 1.0 Hz, 1 H). ^{13}C NMR (CDCl$_3$); δ 21.47, 52.88, 78.58, 80.70, 119.94, 124.82, 126.11, 126.78, 127.76, 128.22, 128.31, 128.68, 128.75, 129.81, 131.13, 132.73, 133.80, 139.79, 162.32, 164.91, and 166.24. HRMS (m/z): [M + H]$^+$ calcd for C$_{23}$H$_{16}$ClN$_2$O$_3$S, 435.0565; found, 435.0570.

4-(5-(Naphthalen-1-yl)-1,3,4-oxadiazol-2-ylthio)but-2-ynyl 4-Methoxybenzoate (34). LC-MS: rt (min) = 7.03. ^{1}H NMR (CDCl$_3$) δ 3.84 (s, 3 H), 4.18 (t, J = 2.1 Hz, 2 H), 4.92 (t, J = 2.1 Hz, 2 H), 6.87 (m, 2 H), 7.58 (m, 2 H), 7.68 (ddd, J = 8.6, 6.9, and 1.6 Hz, 1 H), 7.97 (m, 4 H), 8.14 (dd, J = 7.2 and 1.2 Hz, 1 H) and 9.20 (d, J = 8.6 Hz, 1 H). ^{13}C NMR (CDCl$_3$) δ 21.54, 52.40, 55.42, 79.12, 80.20, 105.02, 113.64, 119.99, 121.72, 124.85, 126.15, 126.75, 128.19, 128.33, 128.65, 129.84, 131.85, 132.69, 133.80, 162.42, 165.50, and 166.19. HRMS (m/z): [M + H]$^+$ calcd for C$_{24}$H$_{19}$N$_2$O$_4$, 431.1060; found, 431.1064.

4-(5-Phenyl-1,3,4-oxadiazol-2-ylthio)but-2-ynyl 4-Fluorobenzoate (44). LC-MS: rt (min) = 6.65. ^{1}H NMR (CDCl$_3$) δ 4.12 (t, J = 2.1 Hz, 2 H), 4.92 (t, J = 2.1 Hz, 2 H), 7.03−7.12 (m, 2 H), 7.43−7.55 (m, 3 H), and 7.94−8.07 (m, 4 H). ^{13}C NMR (CDCl$_3$) δ 21.46, 52.74, 78.62, 80.51, 115.46, 115.67, 123.41, 125.56, 125.59, 126.68, 129.02, 131.77, 132.30, 132.40, 162.50, 164.64, 164.74, 166.18, and 167.17. HRMS (m/z): [M + H]$^+$ calcd for C$_{19}$H$_{14}$FN$_2$O$_3$S, 369.0709; found, 369.0710.

4-(5-(2-Fluorophenyl)-1,3,4-oxadiazol-2-ylthio)but-2-ynyl 4-Fluorobenzoate (45). LC-MS: rt (min) = 6.55. ^{1}H NMR (CDCl$_3$) δ 4.13 (t, J = 2.1 Hz, 2 H), 4.92 (t, J = 2.2 Hz, 2 H), 7.05−7.14 (m, 1 H), 7.17−7.25 (m, 1 H), 7.27−7.33 (m, 1 H), 7.49−7.57 (m, 1 H), and 7.98−8.09 (m, 3 H). ^{13}C NMR (CDCl$_3$) δ 21.48, 52.78, 78.69, 80.47, 111.93, 112.05, 115.49, 115.71, 116.15, 116.37, 116.88, 117.08, 124.63, 124.67, 124.99, 125.60, 125.63,

129.53, 132.34, 132.43, 133.24, 133.34, 133.55, 133.63, 158.55, 161.13, 162.94, 163.14, 164.68, 164.79, 165.43, 167.21, and 167.99. HRMS (m/z): [M + H]$^+$ calcd for $C_{19}H_{13}F_2N_2O_3S$, 387.0615; found, 387.0610.

4-(5-(3-Fluorophenyl)-1,3,4-oxadiazol-2-ylthio)but-2-ynyl 4-Fluorobenzoate (46). LC-MS: rt (min) = 6.74. ^{1}H NMR (CDCl$_3$) δ 4.13 (t, J = 2.1 Hz, 2 H), 4.92 (t, J = 2.1 Hz, 2 H), 7.06−7.13 (m, 2 H), 7.23 (td, J = 8.4 and 2.6 Hz, 1 H), 7.47 (td, J = 8.1 and 5.6 Hz, 1 H), 7.70 (dt, J = 9.2 and 2.1 Hz, 1 H), 7.80 (d, J = 7.8 Hz, 1 H), and 8.01−8.08 (m, 2 H). ^{13}C NMR (CDCl$_3$) δ 21.50, 52.74, 78.78, 80.39, 113.65, 113.89, 115.49, 115.72, 118.77, 118.98, 122.46, 122.49, 125.24, 125.32, 125.57, 125.60, 130.88, 130.97, 132.33, 132.42, 161.55, 163.05, 164.01, 164.69, 164.76, 165.17, 165.20, and 167.22. HRMS (m/z): [M + H]$^+$ calcd for $C_{19}H_{13}F_2N_2O_3S$, 387.0615; found, 387.0612.

4-(5-(4-Fluorophenyl)-1,3,4-oxadiazol-2-ylthio)but-2-ynyl 4-Fluorobenzoate (47). LC-MS: rt (min) = 6.68. ^{1}H NMR (CDCl$_3$) δ 4.12 (t, J = 2.1 Hz, 2 H), 4.92 (t, J = 2.1 Hz, 2 H), 7.06−7.13 (m, 2 H), 7.14−7.21 (m, 2 H), and 7.97−8.09 (m, 4 H). ^{13}C NMR (CDCl$_3$) δ 21.50, 52.75, 78.70, 80.45, 115.50, 115.73, 116.32, 116.54, 119.78, 119.81, 125.59, 125.62, 128.99, 129.07, 132.33, 132.43, 162.59, 163.53, 164.70, 164.77, 165.40, 166.05, and 167.23. HRMS (m/z): [M + H]$^+$ calcd for $C_{19}H_{13}F_2N_2O_3S$, 387.0615; found, 387.0612.

4-(5-(2-Chlorophenyl)-1,3,4-oxadiazol-2-ylthio)but-2-ynyl 4-Fluorobenzoate (48). LC-MS: rt (min) = 6.80. ^{1}H NMR (CDCl$_3$) δ 4.14 (t, J = 2.1 Hz, 2 H), 4.93 (t, J = 2.1 Hz, 2 H), 7.06−7.14 (m, 2 H), 7.36−7.42 (m, 1 H), 7.46 (td, J = 7.6 and 1.8 Hz, 1 H), 7.51−7.56 (m, 1 H), 7.95 (dd, J = 7.8 and 1.8 Hz, 1 H), and 8.01−8.10 (m, 2 H). ^{13}C NMR (CDCl$_3$) δ 21.48, 52.78, 78.72, 80.46, 115.49, 115.72, 122.76, 127.07, 130.98, 131.26, 132.35, 132.44, 132.47, 133.07, 163.26, 164.54, 164.69, and 164.80. HRMS (m/z): [M + H]$^+$ calcd for $C_{19}H_{13}ClFN_2O_3S$, 403.0319; found, 403.0317.

4-(5-(4-Chlorophenyl)-1,3,4-oxadiazol-2-ylthio)but-2-ynyl 4-Fluorobenzoate (49). LC-MS: rt (min) = 7.00. ^{1}H NMR (CDCl$_3$) δ 4.13 (t, J = 2.1 Hz, 2 H), 4.92 (t, J = 2.1 Hz, 2 H), 7.06−7.14 (m, 2 H), 7.46 (m, 2 H), 7.94 (m, 2 H) and 8.01−8.07 (m, 2 H). ^{13}C NMR (CDCl$_3$) δ 21.50, 52.73, 78.73, 80.41, 115.50, 115.72, 121.90, 125.56, 125.59, 127.97, 129.46, 132.33, 132.41, 138.10, 162.82, 164.69, 164.76, 165.39, and 167.23. HRMS (m/z): [M + H]$^+$ calcd for $C_{19}H_{13}ClFN_2O_3S$, 403.0319; found, 403.0320.

4-(5-(Furan-2-yl)-1,3,4-oxadiazol-2-ylthio)but-2-ynyl 4-Fluorobenzoate (50). LC-MS: rt (min) = 6.22. ^{1}H NMR (DMSO-d_6) δ 4.29 (s, 2 H), 4.97 (s, 2 H), 6.77 (dd, J = 3.4 and 1.7 Hz, 1 H), 7.28−7.40 (m, 3 H), 7.92−8.00 (m, 2 H), and 8.03 (s, 1 H). ^{13}C NMR (DMSO-d_6) δ 21.19, 52.74, 78.36, 81.77, 112.60, 114.76, 115.85, 116.07, 125.48, 132.08, 132.18, 138.08, 147.06, 158.35, 161.67, 163.96, and 166.49. HRMS (m/z): [M + H]$^+$ calcd for $C_{17}H_{12}FN_2O_4S$, 359.0502; found, 359.0500.

4-(5-(Thiophen-2-yl)-1,3,4-oxadiazol-2-ylthio)but-2-ynyl 4-Fluorobenzoate (51). LC-MS: rt (min) = 6.48. ^{1}H NMR (CDCl$_3$) δ 4.10 (t, J = 1.8 Hz, 2 H), 4.91 (t, J = 2.2 Hz, 2 H), 7.07−7.15 (m, 3 H), 7.53 (dd, J = 4.8 and 1.2 Hz, 1 H), 7.70 (dd, J = 3.6 and 1.2 Hz, 1 H), and 8.03−8.06 (m, 2 H). ^{13}C NMR (CDCl$_3$); δ 21.5, 52.7, 76.7, 77.0, 77.3, 78.7, 80.4, 115.5, 115.7, 124.6, 125.5, 125.6, 128.1, 129.8, 130.2, 132.3, 132.4, 161.9, 162.4, 164.6, 164.7, and 167.2. HRMS (m/z): [M + H]$^+$ calcd for $C_{17}H_{12}FN_2O_3S_2$, 375.0271; found, 375.0267.

4-(5-(2-Methoxyphenyl)-1,3,4-oxadiazol-2-ylthio)but-2-ynyl 4-Fluorobenzoate (52). LC-MS: rt (min) = 6.40. ^{1}H NMR (CDCl$_3$) δ 3.95 (s, 3 H), 4.12 (t, J = 2.2 Hz, 2 H), 4.92 (t, J = 2.2 Hz, 2 H), 7.01−7.13 (m, 4 H), 7.49 (ddd, J = 8.6, 7.3, and 1.8 Hz, 1 H), 7.87 (dd, J = 7.9 and 1.5 Hz, 1 H), and 8.02−8.08 (m, 2 H). ^{13}C NMR (CDCl$_3$) δ 21.43, 52.81, 55.95, 78.51, 80.67, 111.91, 112.58, 115.48, 115.70, 120.72, 125.62, 125.65, 130.27, 132.34, 132.43, 133.18, 157.76, 162.19, 164.67, 164.80, 164.94, and 167.21. HRMS (m/z): [M + H]$^+$ calcd for $C_{20}H_{16}FN_2O_4S$, 399.0815; found, 399.0820.

4-(5-(3-Hydroxynaphthalen-2-yl)-1,3,4-oxadiazol-2-ylthio)-but-2-ynyl 4-Fluorobenzoate (53). LC-MS: rt (min) = 6.50. ^{1}H NMR (DMSO-d_6) δ 4.07 (s, 2 H), 4.19 (t, J = 2.1 Hz, 2 H), 7.44−7.53 (m, 2 H), 7.64−7.77 (m, 2 H), 8.04 (d, J = 8.0 Hz, 1 H), 8.10 (s, 1 H), 8.19−8.23 (m, 1 H), 8.25−8.31 (m, 2 H), and 8.79 (s, 1 H). ^{13}C NMR (DMSO-d_6) δ 21.07, 48.97, 78.42, 84.04, 115.48, 116.05, 116.27, 121.87, 125.55, 125.58, 127.30, 127.42, 128.84, 129.16, 130.36, 130.61, 132.98, 133.08, 134.42, 144.24, 162.69, 162.83, 164.14, 164.30, and 166.82. HRMS (m/z): [M + H]$^+$ calcd for $C_{23}H_{16}FN_2O_4S$, 435.0814; found, 435.0812.

4-(5-(1H-indol-2-yl)-1,3,4-oxadiazol-2-ylthio)but-2-ynyl 4-Fluorobenzoate (54). LC-MS: rt (min) = 6.26. ^{1}H NMR (400 MHz, DMSO-d_6) δ 4.29 (t, J = 2.1 Hz, 2 H), 4.98 (t, J = 2.1 Hz, 2 H), 7.19−7.30 (m, 3 H), 7.53 (dd, J = 6.9 and 1.5 Hz, 1 H), 7.87−7.95 (m, 2 H), 8.02−8.09 (m, 1 H), 8.16 (d, J = 2.9 Hz, 1 H), and 12.03 (brs, 1 H). ^{13}C NMR (DMSO-d_6) δ 21.13, 52.78, 78.19, 82.10, 99.02, 112.43, 115.74, 115.96, 120.10, 121.24, 122.87, 123.87, 128.40, 132.01, 132.10, 136.39, 159.20, 163.51, and 163.96. HRMS (m/z): [M + H]$^+$ calcd for $C_{21}H_{15}FN_3O_3S$, 408.0818; found, 408.0813.

4-(5-(Quinolin-5-yl)-1,3,4-oxadiazol-2-ylthio)but-2-ynyl 4-Fluorobenzoate (55). LC-MS: rt (min) = 5.60. ^{1}H NMR (DMSO-d_6) δ 4.38 (t, J = 2.1 Hz, 2 H), 4.98 (t, J = 2.0 Hz, 2 H), 7.14−7.23 (m, 2 H), 7.77 (dd, J = 8.7 and 4.2 Hz, 1 H), 7.81−7.88 (m, 2 H), 7.92 (dd, J = 8.5 and 7.3 Hz, 1 H), 8.23−8.31 (m, 2 H), 9.06 (dd, J = 4.2 and 1.7 Hz, 1 H), and 9.41−9.48 (m, 1 H). ^{13}C NMR (DMSO-d_6) δ 21.02, 52.72, 78.37, 81.96, 115.68, 115.90, 119.70, 123.12, 124.52, 128.74, 129.22, 131.90, 132.00, 133.13, 134.21, 147.21, 151.07, 162.55, 163.83, 164.58, and 166.34.

4-(5-(Naphthalen-1-yl)-1,3,4-oxadiazol-2-ylthio)butyl 4-Fluoro-benzoate (61). LC-MS: rt (min) = 7.39. ^{1}H NMR (CDCl$_3$) δ 1.92−2.18 (m, 4 H), 3.44 (td, J = 7.1 and 2.8 Hz, 2 H), 4.36−4.46 (m, 2 H), 7.04−7.14 (m, 2 H), 7.52−7.64 (m, 2 H), 7.66−7.74 (m, 1 H), 7.93 (d, J = 8.2 Hz, 1 H), 7.99−8.10 (m, 3 H), 8.10−8.18 (m, 1 H), and 9.21 (d, J = 8.6 Hz, 1 H). ^{13}C NMR NMR (CDCl$_3$) δ 26.11, 27.74, 32.15, 64.25, 115.41, 115.64, 120.12, 124.83, 126.17, 126.38, 126.73, 128.14, 128.66, 129.83, 132.06, 132.15, 132.55, 133.82, 163.97, 164.49, 165.56, 165.76, and 167.01. HRMS (m/z): [M + H]$^+$ calcd for $C_{23}H_{20}FN_2O_3S$, 423.1178; found, 423.1176.

4-((5-(Naphthalen-1-yl)-1,3,4-oxadiazol-2-ylthio)methyl)-benzyl 4-Fluorobenzoate (62). LC-MS: rt (min) = 7.59. ^{1}H NMR (CDCl$_3$) δ 4.59 (s, 2 H), 5.35 (s, 2 H), 7.06−7.14 (m, 2 H), 7.44 (d, J = 8.0 Hz, 2 H), 7.51−7.63 (m, 4 H), 7.65−7.72 (m, 1 H), 7.93 (d, J = 8.0 Hz, 1 H), 8.03 (d, J = 8.0 Hz, 1 H), 8.05−8.13 (m, 3 H), and 9.19 (d, J = 8.6 Hz, 1 H). ^{13}C NMR NMR (CDCl$_3$) δ 36.41, 66.35, 115.44, 115.66, 120.08, 124.82, 126.16, 126.22, 126.25, 126.73, 128.14, 128.19, 128.64, 129.48, 129.82, 132.21, 132.30, 132.58, 133.81, 135.87, 135.93, 163.50, 164.57, 165.39, 165.89, and 167.10. HRMS (m/z): [M + H]$^+$ calcd for $C_{27}H_{20}FN_2O_3S$, 471.1178; found, 471.1175.

Methods. Biological Reagents. All commercial fatty acids (Sigma-Aldrich Chemical Co.) were repurified using a Higgins HAIsil Semi-Preparative (5 μm, 250 mm × 10 mm) C-18 column. Solution A was 99.9% MeOH and 0.1% acetic acid; solution B was 99.9% H$_2$O and 0.1% acetic acid. An isocratic elution of 85% A:15% B was used to purify all fatty acids, which were stored at −80 °C for a maximum of 6 months. LO products were generated by reacting substrate with the appropriate LO isozyme (13-HPODE from sLO-1 and LA, 13-HPOTrE from sLO-1 and ALA, 15-HPETE from sLO-1 and AA, and 12-HPETE from 12-hLO and AA). Product generation was per-formed as follows. An assay of 100 mL of 50−100 μM substrate was run to completion, reactions were quenched with 5 mL acetic acid, extracted twice with 50 mL of dichloromethane, evaporated to dryness, and reconstituted in MeOH for HPLC purification. All products were tested with sLO-1 to show that no residual substrate was present, and demonstrated, by both analytical HPLC and LC/MS/MS, to have greater than 98% purity.

The reduced products were generated by selectively reducing the 98% pure peroxide product to the alcohol, with trimethylphosphite. The purity of the reduced hydroxy products was then confirmed with LC-MS/MS. All other chemicals were reagent grade or better and were used without further purification.

Overexpression and Purification of 15-Human Lipoxygenase-1 and 12-Human Lipoxygenase. Human reticulocyte 15-lipoxygenase-1 (15-hLO-1), human epithelial 15-lipoxygenase-2 (15-hLO-2), and human platelet 12-lipoxygenase (12-hLO) were expressed as *N*-terminally, His$_6$-tagged proteins and purified to greater than 90% purity, as evaluated by SDS-PAGE analysis.[27c,54,46] Human 5-lipoxygenase was expressed as a nontagged protein and used as a crude ammonium sulfate protein fraction, as published previously.[47] Iron content of 15-hLO-1 was determined with a Finnigan inductively coupled plasma mass spectrometer (ICP-MS), using cobalt-EDTA as an internal standard. Iron concentrations were compared to standardized iron solutions and used to normalize enzyme concentrations.

High-Throughput Screen: Materials. Dimethyl sulfoxide (DMSO) ACS grade was from Fisher, while ferrous ammonium sulfate, Xylenol Orange (XO), sulfuric acid, and Triton X-100 were obtained from Sigma-Aldrich.

Compound Library. A 74290 compound library was screened in 7−15 concentrations ranging from 0.7 nM to 57 μM. The library included 61548 diverse small drug-like molecules that are part of the NIH Small Molecule Repository. A collection of 1372 compounds from the Centers of Methodology and Library Development at Boston University (BUCMLD) and University of Pittsburgh (UPCMLD) were added to the library. Several combinatorial libraries from Pharmacopeia, Inc., totaled 2419 compounds. An additional 1963 compounds from the NCI Diversity Set were included. Last, 6925 compounds with known pharmacological activity were added to provide a large and diverse screening collection.

High-Throughput Screening Protocol and HTS Analysis. All screening operations were performed on a fully integrated robotic system (Kalypsys Inc., San Diego, CA) as described elsewhere.[48] First, 3 μL of enzyme (40 nM 15-hLO-1, final concentration) was dispensed into a 1536-well Greiner black clear-bottom assay plate. Then compounds and controls (23 nL) were transferred via Kalypsys PinTool equipped with 1536-pin array. The plate was incubated for 15 min at room temperature, and then a 1 μL aliquot of substrate solution (50 μM arachidonic acid final concentration) was added to start the reaction. The reaction was stopped after 6.5 min by the addition of 4 μL of FeXO solution (final concentrations of 200 μM Xylenol Orange (XO) and 300 μM ferrous ammonium sulfate in 50 mM sulfuric acid). After a short spin (1000 rpm, 15 s), the assay plate was incubated at room temperature for 30 min. The absorbances at 405 and 573 nm were recorded using ViewLux high throughput CCD imager (Perkin-Elmer, Waltham, MA) using standard absorbance protocol settings. During dispensing, enzyme and substrate bottles were kept submerged into +4 °C recirculating chiller bath to minimize degradation. Plates containing DMSO only (instead of compound solutions) were included approximately every 50 plates throughout the screen to monitor any systematic trend in the assay signal associated with reagent dispenser variation or decrease in enzyme specific activity.

Data were analyzed in a similar method as described elsewhere.[42] Briefly, assay plate-based raw data were normalized to controls and plate-based data corrections were applied to filter out background noise. All concentration−response curves (CRCs) were fitted using in-house developed software (http://ncgc.nih.gov/pub/openhts/). Curves were categorized into four classes: complete response curves (Class 1), partial curves (Class 2), single point actives (Class 3), and inactives (Class 4). Compounds with the highest quality, Class 1 and Class 2 curves, were prioritized for follow-up.

Lipoxygenase UV−vis Assay. The initial one-point inhibition percentages were determined by following the formation of the conjugated diene product at 234 nm ($\varepsilon = 25000$ M^{-1}cm^{-1}) with a Perkin-Elmer Lambda 40 UV−vis spectrophotometer at one inhibitor concentration. All reactions were 2 mL in volume and constantly stirred using a magnetic stir bar at room temperature (23 °C) with approximately 40 nM for 12-hLO, 20 nM of 15-hLO-1 (by iron content), and 1 μM for 15-hLO-2. Reactions with the crude, ammonium sulfate precipitated 5-hLO were carried out in 25 mM HEPES (pH 7.3), 0.3 mM CaCl$_2$, 0.1 mM EDTA, 0.2 mM ATP, 0.01% Triton X-100, 10 μM AA and with 12-hLO in 25 mM Hepes buffer (pH 8), 0.01% Triton X-100, and 10 μM AA. Reactions with 15-hLO-1 and 15-hLO-2 were carried out in 25 mM Hepes buffer (pH 7.5), 0.01% Triton X-100, and 10 μM AA. The concentration of AA (for 5-hLO, 12-hLO, and 15-hLO-2) and LA (for 15-hLO-1) were quantitatively determined by allowing the enzymatic reaction to go to completion. IC$_{50}$ values were obtained by determining the enzymatic rate at various inhibitor concentrations and plotted against inhibitor concentration, followed by a hyperbolic saturation curve fit (assuming total enzyme concentration [E] $\ll K_i^{app}$, so IC$_{50} \sim K_i^{app}$). It should be noted that all of the potent inhibitors displayed greater than 80% maximal inhibition unless stated in the tables. For a number of inhibitors, the K_i^{app} value approached the total active enzyme concentration ([E]), indicating that hyperbolic fitting of the data was inappropriate. The K_i^{app} values were then determined by plotting the fractional velocity as a function of the inhibitor concentration, followed by a quadratic fit using the Morrison equation.[49] To determine the average K_i^{app} and the associated error, the enzyme concentration in the Morrison equation was varied from the maximal [E] (as measured by the metal content) to 0.01 nM. It should be noted that the total active enzyme concentration ([E]) depends on the iron content and varies with enzyme preparation. The subsequent K_i^{app} values were averaged and the standard deviation determined. Inhibitors that displayed a standard deviation in K_i^{app} less than 50% are presented in the tables with their standard deviation, whereas compounds with greater than 50% standard deviation in their K_i^{app} were considered beyond the limit of our assay and thus the maximal K_i^{app} value was set to half the [E], or < 10 nM. Inhibitors were stored at −20 °C in DMSO.

Lag-Phase Kinetic Analysis. The lag-phase of 15-hLO-1 was examined with the addition of compounds **5**, **13**, **39**, and **44** with our standard kinetic analysis (*vide supra*). Inhibitor concentrations were varied and the reactions allowed to progress for an extensive period of time in order to determine if the inhibitory lag-phase could be overcome. If the mechanism of the inhibitor is reductive, it is common to see resumption of enzyme activity after a period of time due to the destruction of the inhibitor by the pseudoperoxidase activity of the LO.[50]

DPPH Antioxidant Test. Compounds **22** and **30** were dissolved in dimethyl sulfoxide (DMSO) at 1−20 mM concentration (1000-fold concentrated). The antioxidant activity of these compounds was assayed by monitoring the quenching of the standard free radical 1.1-diphenyl-2-picrylhydrazyl (DPPH) upon reaction with the testing compounds.[51,52] A known free radical scavenger, nordihydroguaiaretic acid (NDGA), was used as a positive control. Ten μL of 1 mM testing reagents to achieve a final concentration of 5 μM was added to 2 mL of 500 μM DPPH, stirring in a cuvette. Optical absorbance was monitored and recorded at 25 s intervals as described elsewhere.[51,52] The decrease in optical absorbance at 517 nm was monitored using a P-E Lambda 40 spectrometer. The rate of reaction is proportional to the antioxidant potency of the test compounds.

Reversibility of Inhibition. Three separate 1 mL samples of 15-hLO-1 were incubated with 10 μL of **25** (final concentration of 50 μM), **33** (final concentration of 50 μM), and DMSO followed by dialysis in 25 mM HEPES, 150 mM NaCl, and 10% glycerol at pH 7.5 for 2 h. Activity was recorded by monitoring the formation of the conjugated product before and after the dialysis.

Steady-State Inhibition Kinetics. Lipoxygenase rates were determined by monitoring the formation of the conjugated product, 15-HPETE, at 234 nm ($\varepsilon = 25\,000$ M^{-1} cm^{-1}) with a Perkin-Elmer Lambda 40 UV/vis spectrophotometer. Reactions were initiated by adding approximately 80 nM 15-hLO-1 to a constantly stirring 2 mL cuvette containing $3-40\,\mu$M AA in 25 mM HEPES buffer (pH 7.5) in the presence of 0.01% Triton X-100. The substrate concentration was quantitated by allowing the enzymatic reaction to proceed to completion. Kinetic data were obtained by recording initial enzymatic rates, at varied inhibitor concentrations, and subsequently fitted to the Henri–Michaelis–Menten equation, using KaleidaGraph (Synergy) to determine the microscopic rate constants, V_{max} (μmol/min/mg) and V_{max}/K_M (μmol/min/mg/μM). These rate constants were subsequently replotted, $1/V_{max}$ and K_M/V_{max} versus inhibitor concentration, to yield K_i' and K_i, respectively.

Allosteric Inhibition. To assess if this chemotype affected the substrate specificity by binding to the allosteric site, we performed the competitive substrate capture method, as previously described.[3d] Briefly, 15-hLO-1 was allowed to react with a mixture of AA and LA and the product ratio determined by HPLC. This experiment was repeated with inhibitor present and the product ratio compared.

Cyclooxygenase Assay. Ovine COX-1 (cat. no. 60100) and human COX-2 (cat. no. 60122) were purchased from Cayman Chemical. Approximately 2 μg of either COX-1 or COX-2 were added to buffer containing 100 μM AA, 0.1 M Tris-Hcl buffer (pH 8.0), 5 mM EDTA, 2 mM phenol, and 1 μM hematin at 37 °C. Data was collected using a Hansatech DW1 oxygen electrode chamber. Inhibitors were incubated with the respective COX for 20 min and added to the reaction mixture, and the consumption of oxygen was recorded. Ibuprofen and the carrier solvent, DMSO, were used as positive and negative controls, respectively.

Supporting Information Available: Additional experimental procedures and spectroscopic data (^{1}H NMR, LC/MS, and HRMS) for representative compounds; qHTS assay performance figures. This material is available free of charge via the Internet at http://pubs.acs.org.

References

(1) Solomon, E. I.; Zhou, J.; Neese, F.; Pavel, E. G. New insights from spectroscopy into the structure/function relationships of lipoxygenases. *Chem. Biol.* **1997**, *4*, 795–808.

(2) Brash, A. R. Lipoxygenases: Occurrence, Functions, Catalysis and Acquisition of Substrate. *J. Biol. Chem.* **1999**, *274*, 23679–23682.

(3) (a) Whitman, S.; Gezginci, M.; Timmermann, B. N.; Holman, T. R. Structure–activity relationship studies of nordihydroguaiaretic acid inhibitors toward soybean, 12-human, and 15-human lipoxygenase. *J. Med. Chem.* **2002**, *45*, 2659–2661. (b) Berger, W.; De Chandt, M. T.; Cairns, C. B. Zileuton: clinical implications of 5-lipoxygenase inhibition in severe airway disease. *Int. J. Clin. Pract.* **2007**, *61*, 663–676. (c) Mogul, R.; Johansen, E.; Holman, T. R. Oleyl sulfate reveals allosteric inhibition of soybean lipoxygenase-1 and human 15-lipoxygenase. *Biochemistry* **2000**, *39*, 4801–4807. (d) Wecksler, A. T.; Kenyon, V.; Deschamps, J. D.; Holman, T. R. Substrate specificity changes for human reticulocyte and epithelial 15-lipoxygenases reveal allosteric product regulation. *Biochemistry* **2008**, *47*, 7364–7375. (e) Steele, V. E.; Holmes, C. A.; Hawk, E. T.; Kopelovich, L.; Lubet, R. A.; Crowell, J. A.; Sigman, C. C.; Kelloff, G. J. Lipoxygenase inhibitors as potential cancer chemopreventives. *Cancer Epidemiol. Biomarkers Prev.* **1999**, *8*, 467–483.

(4) Samuelsson, B.; Dahlen, S. E.; Lindgren, J. A.; Rouzer, C. A.; Serhan, C. N. Leukotrienes and Lipoxins: Structures, Biosynthesis, and Biological Effects. *Science* **1987**, *237*, 1171–1176.

(5) Ford-Hutchinson, A. W.; Gresser, M.; Young, R. N. 5-Lipoxygenase. *Annu. Rev. Biochem.* **1994**, *63*, 383–417.

(6) Kuhn, H.; Chaitidis, P.; Roffeis, J.; Walther, M. Arachidonic acid metabolites in the cardiovascular system: the role of lipoxygenase isoforms in atherogenesis with particular emphasis on vascular remodeling. *J. Cardiovasc. Pharmacol.* **2007**, *50*, 609–620.

(7) Murphy, R. C.; Gijon, M. A. Biosynthesis and metabolism of leukotrienes. *Biochem. J.* **2007**, *405*, 379–395.

(8) Ghosh, J.; Myers, C. E. Inhibition of arachidonate 5-lipoxygenase triggers massive apoptosis in human prostate cancer cells. *Proc. Natl. Acad. Sci. U.S.A* **1998**, *95*, 13182–13187.

(9) Nakano, H.; Inoue, T.; Kawasaki, N.; Miyataka, H.; Matsumoto, H.; Taguchi, T.; Inagaki, N.; Nagai, H.; Satoh, T. Synthesis and biological activities of novel antiallergic agents with 5-lipoxygenase inhibiting action. *Bioorg. Med. Chem.* **2000**, *8*, 373–380.

(10) Dailey, L. A.; Imming, P. 12-Lipoxygenase: classification, possible therapeutic benefits from inhibition, and inhibitors. *Curr. Med. Chem.* **1999**, *6*, 389–398.

(11) Hussain, H.; Shornick, L. P.; Shannon, V. R.; Wilson, J. D.; Funk, C. D.; Pentland, A. P.; Holtzman, M. J. Epidermis Contains Platlet-Type 12-Lipoxygenase that is Overexpressed in Germinal Layer Keratinocytes in Psoriasis. *Am. J. Physiol.* **1994**, *266*, C243–C253.

(12) Ding, X. Z.; Iversen, P.; Cluck, M. W.; Knezetic, J. A.; Adrian, T. E. Lipoxygenase inhibitors abolish proliferation of human pancreatic cancer cells. *Biochem. Biophys. Res. Commun.* **1999**, *261*, 218–223.

(13) Connolly, J. M.; Rose, D. P. Enhanced angiogenesis and growth of 12-LO gene-transfected MCF-7 human breast cancer cells in athymic nude mice. *Cancer Lett.* **1998**, *132*, 107–112.

(14) Natarajan, R.; Nadler, J. Role of lipoxygenases in breast cancer. *Front. Biosci.* **1998**, *3*, E81–88.

(15) Shappell, S. B.; Manning, S.; Boeglin, W. E.; Guan, Y. F.; Roberts, R. L.; Davis, L.; Olson, S. J.; Jack, G. S.; Coffey, C. S.; Wheeler, T. M.; Breyer, M. D.; Brash, A. R. Alterations in lipoxygenase and cyclooxygenase-2 catalytic activity and mRNA expression in prostate carcinoma. *Neoplasia* **2001**, *3*, 287–303.

(16) Nie, D.; Hillman, G. G.; Geddes, T.; Tang, K.; Pierson, C.; Grignon, D. J.; Honn, K. V. Platelet-type 12-LO in a human prostate carcinoma stimulates angiogenesis and tumor growth. *Cancer Res.* **1998**, *58*, 4047–4051.

(17) Schewe, T. 15-Lipoxygenase-1: a prooxidant enzyme. *Biol. Chem.* **2002**, *383*, 365–374.

(18) Shappell, S. B.; Olson, S. J.; Hannah, S. E.; Manning, S.; Roberts, R. L.; Masumori, N.; Jisaka, M.; Boeglin, W. E.; Vader, V.; Dave, D. S.; Shook, M. F.; Thomas, T. Z.; Funk, C. D.; Brash, A. R. Elevated expression of 12/15-lipoxygenase and cyclooxygenase-2 in a transgenic mouse model of prostate carcinoma. *Cancer Res.* **2003**, *63*, 2256–2267.

(19) Hsi, L. C.; Wilson, L. C.; Eling, T. E. Opposing effects of 15-lipoxygenase-1 and -2 metabolites on MAPK signaling in prostate. Alteration in peroxisome proliferator-activated receptor gamma. *J. Biol. Chem.* **2002**, *277*, 40549–40556.

(20) Kelavkar, U. P.; Cohen, C.; Kamitani, H.; Eling, T. E.; Badr, K. F. Concordant induction of 15-lipoxygenase-1 and mutant p53 expression in human prostate adenocarcinoma: correlation with Gleason staging. *Carcinogenesis* **2000**, *21*, 1777–1787.

(21) Suraneni, M. V.; Schneider-Broussard, R.; Moore, J. R.; Davis, T. C.; Maldonado, C. J.; Li, H.; Newman, R. A.; Kusewitt, D.; Hu, J.; Yang, P.; Tang, D. G. Transgenic expression of 15-lipoxygenase 2 (15-LOX2) in mouse prostate leads to hyperplasia and cell senescence. *Oncogene* **2010**, *29*, 4261–4275.

(22) Wu, Y.; Fang, B.; Yang, X. Q.; Wang, L.; Chen, D.; Krasnykh, V.; Carter, B. Z.; Morris, J. S.; Shureiqi, I. Therapeutic molecular targeting of 15-lipoxygenase-1 in colon cancer. *Mol. Ther.* **2008**, *16*, 886–892.

(23) Andersson, C. K.; Claesson, H.-K.; Rydell-Toermaenen, K.; Swedmark, S.; Haellgren, A.; Eriefaelt, J. S. Mice lacking 12/15-liopygenase have attenuated airway allergic inflammation and remodeling. *Am. J. Respir. Cell Mol. Biol.* **2008**, *39*, 648–656.

(24) Chawengsub, Y.; Gauthier, K. M.; Campbell, W. B. Role of arachidonic acid lipoxygenase metabolites in the regulation of

vascular tone. *Am. J. Physiol. Heart Circ. Physiol.* **2009**, *297*, H495–H507.

(25) Chan, P. H. Role of oxidants in ischemic brain damage. *Stroke* **1996**, *27*, 1124–1129.

(26) Pallast, S.; Arai, K.; Wang, X.; Lo, E. H.; van Leyen, K. 12/15-Lipoxygenase targets neuronal mitochondria under oxidative stress. *J. Neurochem.* **2009**, *111*, 882–889.

(27) (a) Deschamps, J. D.; Kenyon, V. A.; Holman, T. R. Baicalein is a potent in vitro inhibitor against both reticulocyte 15-human and platelet 12-human lipoxygenases. *Bioorg. Med. Chem.* **2006**, *14*, 4295–4301. (b) Segraves, E. N.; Shah, R. R.; Segraves, N. L.; Johnson, T. A.; Whitman, S.; Sui, J. K.; Kenyon, V. A.; Cichewicz, R. H.; Crews, P.; Holman, T. R. Probing the activity differences of simple and complex brominated aryl compounds against 15-soybean, 15-human, and 12-human lipoxygenase. *J. Med. Chem.* **2004**, *47*, 4060–4065. (c) Amagata, T.; Whitman, S.; Johnson, T.; Stessmann, C. C.; Carroll, J.; Loo, C.; Clardy, J.; Lobkovsky, E.; Crews, P.; Holman, T. R. Sponge Derived Terpenoids with Selectivity towards Human 15-Lipoxygenase versus Human 12-Lipoxygenase. *J. Nat. Prod.* **2003**, *66*, 230–235. (d) Cichewicz, R. H.; Kenyon, V. A.; Whitman, S.; Morales, N. M.; Arguello, J. F.; Holman, T. R.; Crews, P. Redox inactivation of human 15-lipoxygenase by marine-derived meroditerpenes and synthetic chromanes: archetypes for a unique class of selective and recyclable inhibitors. *J. Am. Chem. Soc.* **2004**, *126*, 14910–14920. (e) Vasquez-Martinez, Y.; Ohri, R. V.; Kenyon, V.; Holman, T. R.; Sepulveda-Boza, S. Structure–activity relationship studies of flavonoids as potent inhibitors of human platelet 12-hLO, reticulocyte 15-hLO-1, and prostate epithelial 15-hLO-2. *Bioorg. Med. Chem.* **2007**, *15*, 7408–7425.

(28) Sailer, E. R.; Schweizer, S.; Boden, S. E.; Ammon, H. P. T.; Safayhi, H. Characterization of an acetyl-11-keto-B-boswellic acid and arachidonate-binding regulatory site of 5-lipoxygenase using photoaffinity labeling. *Eur. J. Biochem.* **1998**, *256*, 364–368.

(29) Malterud, K. E.; Rydland, K. M. Inhibitors of 15-lipoxygenase from orange peel. *J. Agric. Food Chem.* **2000**, *48*, 5576–5580.

(30) Moreau, R. A.; Agnew, J.; Hicks, K. B.; Powell, M. J. Modulation of lipoxygenase activity by bacterial hopanoids. *J. Nat. Prod.* **1997**, *60*, 397–398.

(31) Togola, A.; Hedding, B.; Theis, A.; Wangensteen, H.; Rise, F.; Smestad Paulsen, B.; Diallo, D.; Egil Malterud, K. 15-Lipoxygenase inhibitory effects of prenylated flavonoids from *Erythrina senegalensis*. *Planta Med.* **2009**, *75*, 1168–1170.

(32) Sadeghian, H.; Attaran, N.; Jafari, Z.; Saberi, M. R.; Pordel, M.; Riazi, M. M. Design and synthesis of 4-methoxyphenylacetic acid esters as 15-lipoxygenase inhibitors and SAR comparative studies of them. *Bioorg. Med. Chem.* **2009**, *17*, 2327–2335.

(33) Bakavoli, M.; Nikpour, M.; Rahimizadeh, M.; Saberi, M. R.; Sadeghian, H. Design and synthesis of pyrimido[4,5-*b*][1,4]-benzothiazine derivatives, as potent 15-lipoxygenase inhibitors. *Bioorg. Med. Chem.* **2007**, *15*, 2120–2126.

(34) Ohri, R. V.; Radosevich, A. T.; Hrovat, K. J.; Musich, C.; Huang, D.; Holman, T. R.; Toste, F. D. A Re(V)-catalyzed C–N bond-forming route to human lipoxygenase inhibitors. *Org. Lett.* **2005**, *7*, 2501–2504.

(35) Kenyon, V.; Chorny, I.; Carvajal, W. J.; Holman, T. R.; Jacobson, M. P. Novel human lipoxygenase inhibitors discovered using virtual screening with homology models. *J. Med. Chem.* **2006**, *49*, 1356–1363.

(36) Weinstein, D. S.; Liu, W.; Gu, Z.; Langevine, C.; Ngu, K.; Fadnis, L.; Combs, D. W.; Sitkoff, D.; Ahmad, S.; Zhuang, S.; Chen, X.; Wang, F. L.; Loughney, D. A.; Atwal, K. S.; Zahler, R.; Macor, J. E.; Madsen, C. S.; Murugesan, N. Tryptamine and homotryptamine-based sulfonamides as potent and selective inhibitors of 15-lipoxygenase. *Bioorg. Med. Chem. Lett.* **2005**, *15*, 1435–1440.

(37) Weinstein, D. S.; Liu, W.; Ngu, K.; Langevine, C.; Combs, D. W.; Zhuang, S.; Chen, C.; Madsen, C. S.; Harper, T. W.; Robl, J. A. Discovery of selective imidazole-based inhibitors of mammalian 15-lipoxygenase: highly potent against human enzyme within a cellular environment. *Bioorg. Med. Chem. Lett.* **2007**, *17*, 5115–5120.

(38) Also see a recent report of potent 15-hLO-1 inhibitors, however, no chemical structures are provided. Dahlström, M.; Forsström, D.; Johannesson, M.; Huque-Anderson, Y.; Björk, M.; Silfverplatz, E.; Sanin, A.; Schaal, W.; Pelcman, B.; Forsell, P. K. A. Development of a Fluorescent Intensity Assay Amendable for High-Throughput Screening for Determining 15-Lipoxygenase Activity. *J. Biol. Screening* **2010**, *10*, 671–679.

(39) These compounds are a part of the NIH Small Molecule Repository: see http://mlsmr.glpg.com.

(40) (a) Jiang, Z.-Y.; Woollard, A. C. S.; Wolff, S. P. Lipid Hydroperoxide Measurement by Oxidation of Fe^{2+} in the Presence of Xylenol Orange. Comparison with the TBA Assay and an Iodometric Method. *Lipids* **1991**, *26*, 853–856. (b) Deschamps, J. D.; Gautschi, J. T.; Whitman, S.; Johnson, T. A.; Gassner, N. C.; Crews, P.; Holman, T. R. Discovery of platelet-type 12-human lipoxygenase selective inhibitors by high-throughput screening of structurally diverse libraries. *Bioorg. Med. Chem.* **2007**, *15*, 6900–6908.

(41) Eastwood, B. J.; Farmen, M. W.; Iversen, P. W.; Craft, T. J.; Smallwood, J. K.; Garbison, K. E.; Delapp, N. W.; Smith, G. F. The Minimum Significant Ratio: A Statistical Parameter to Characterize the Reproducibility of Potency Estimates from Concentration–Response Assays and Estimation by Replicate-Experiment Studies. *J. Biomol. Screening* **2006**, *11*, 253–261.

(42) Inglese, J.; Auld, D. S.; Jadhav, A.; Johnson, R. L.; Simeonov, A.; Yasgar, A.; Zheng, W.; Austin, C. P. Quantitative high-throughput screening: a titration-based approach that efficiently identifies biological activities in large chemical libraries. *Proc. Natl. Acad. Sci. U.S.A.* **2006**, *103*, 11473–11478.

(43) (a) Gillmor, S. A.; Villasenor, A.; Fletterick, R.; Sigal, E.; Browner, M. F. The structure of mammalian 15-lipoxygenase reveals similarity to the lipases and the determinants of structure specificity. *Nature Struct. Biol.* **1997**, *4*, 1003–1009. (b) Choi, J.; Chon, J.-K.; Kim, S.; Shin, W. Conformational flexibility in mammalian 15S-lipoxygenase: reinterpretation of the crystallographic data. *Proteins: Struct., Funct., Bioinf.* **2008**, *70*, 1023–1032.

(44) Babaoglu, K.; Simeonov, A.; Irwin, J. J.; Nelson, M. E.; Feng, B.; Thomas, C. J.; Cancian, L.; Costi, M. P.; Maltby, D. A.; Jadhav, A.; Inglese, J.; Austin, C. P.; Shoichet, B. K. Comprehensive mechanistic analysis of hits from high-throughput and docking screens against beta-lactamase. *J. Med. Chem.* **2008**, *51*, 2502–2511.

(45) Wecksler, A. T.; Kenyon, V.; Garcia, N. K.; Deschamps, J. D.; van der Donk, W. A.; Holman, T. R. Kinetic and Structural Investigations of the Allosteric Site in Human Epithelial 15-Lipoxygenase-2. *Biochemistry* **2009**, *48*, 8721–8730.

(46) Chen, X.-S.; Brash, A. R.; Funk, C. D. Purification and characterization of recombinant histidine-tagged human platelet 12-lipoxygenase expressed in a baculovirus/insect cell system. *Eur. J. Biochem.* **1993**, *214*, 845–852.

(47) Robinson, S. J.; Hoobler, E. K.; Riener, M.; Loveridge, S. T.; Tenney, K.; Valeriote, F. A.; Holman, T. R.; Crews, P. Using enzyme assays to evaluate the structure and bioactivity of sponge-derived meroterpenes. *J. Nat. Prod.* **2009**, *72*, 1857–1863.

(48) Michael, S.; Auld, D.; Klumpp, C.; Jadhav, A.; Zheng, W.; Thorne, N.; Austin, C. P.; Inglese, J.; Simeonov, A. A Robotic Platform for Quantitative High-Throughput Screening. *Assay Drug Dev. Technol.* **2008**, *6*, 637–658.

(49) Morrison, J. F. Kinetics of the reversible inhibition of enzyme-catalysed reactions by tight-binding inhibitors. *Biochim. Biophys. Acta* **1969**, *185*, 269–286.

(50) Reynolds, C. H. Inactivation of soybean lipoxygenase by lipoxygenase inhibitors in the presence of 15-hydroperoxyeicosatetraenoic acid. *Biochem. Pharmacol.* **1988**, *37*, 4531–4537.

(51) Wang, H.; Li, J.; Follett, P. L.; Zhang, Y.; Cotanche, D. A.; Jensen, F. E.; Volpe, J. J.; Rosenberg, P. A. 12-Lipoxygenase plays a key role in cell death caused by glutathione depletion and arachidonic acid in rat oligodendrocytes. *Eur. J. Neurosci.* **2004**, *20*, 2049–2058.

(52) Van Leyen, K.; Arai, K.; Jin, G.; Kenyon, V.; Gerstner, B.; Rosenberg, P. A.; Holman, T. R.; Lo, E. H. Novel lipoxygenase inhibitors as neuroprotective agents. *J. Neurosci. Res.* **2008**, *86*, 904–909.